



*Economics & Sociology
Reading Room*

**Advance of Irrigation Water on the
Soil Surface In Relation to
Soil Infiltration Rate: A Mathematical
and Laboratory Model Study**

by Mohamed Asseed and Don Kirkham

Department of Agronomy

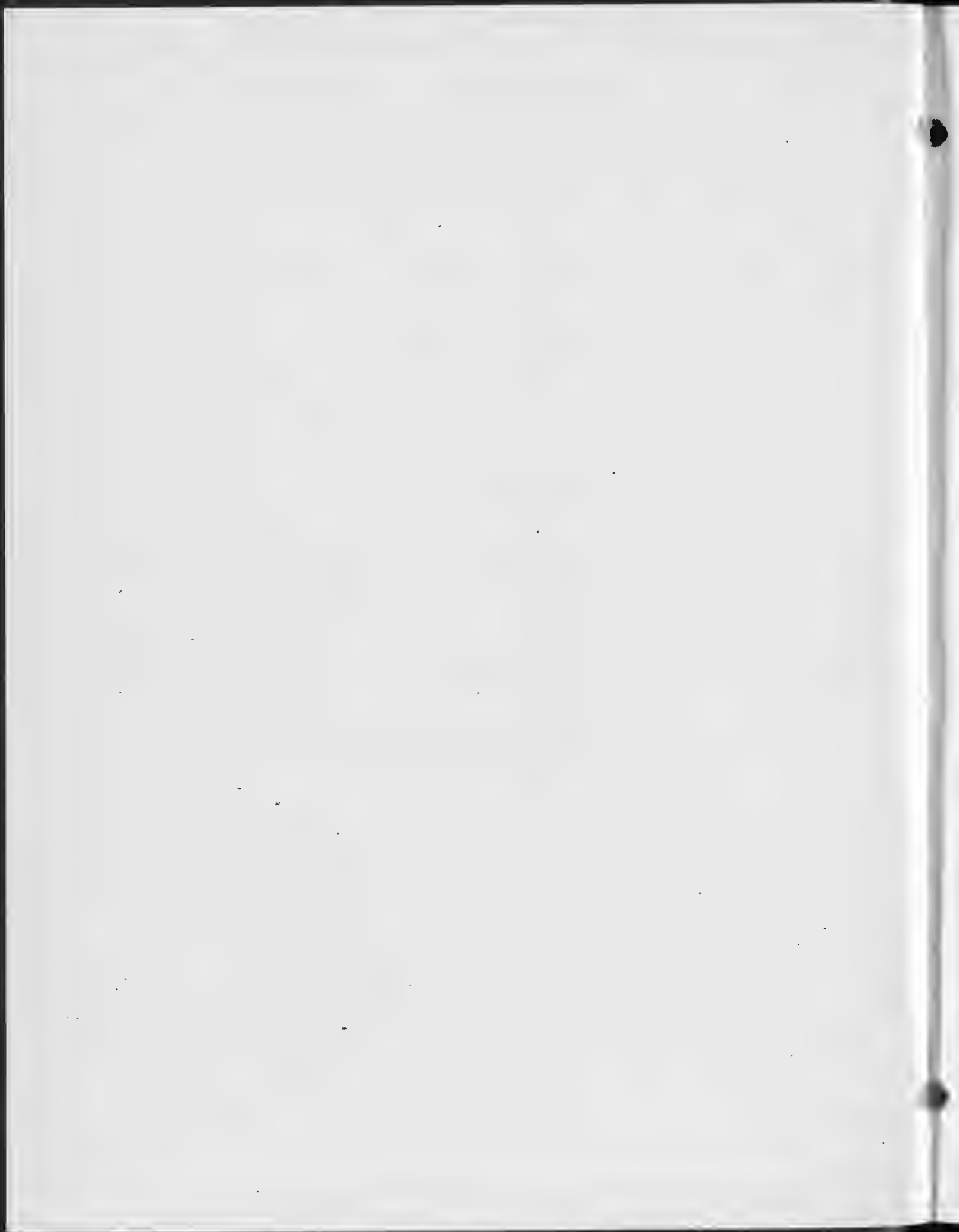
**IOWA AGRICULTURE AND HOME ECONOMICS EXPERIMENT STATION
IOWA STATE UNIVERSITY of Science and Technology**

RESEARCH BULLETIN 565 . . . SEPTEMBER 1968 . . . AMES, IOWA



CONTENTS

Summary	293
Introduction	295
Theory	295
Derivation of the irrigation advance equation	295
Solution for the infiltration case $y = Kt$	296
Solution for the infiltration case $y = Et^a$	297
Solution for the infiltration case $y = At^{1/2} + Bt$	297
Experiment	300
The irrigation model	300
The water-feeding system	300
Porous media used in the model and their infiltration characteristics	300
Experimental procedure	302
Two types of experiments	302
Field infiltration	302
Results	303
Horizontal advance of water in the models with glass beads as porous medium	303
Dimensionless functions for the horizontal advance of irrigation water	305
Moisture profiles in the model during infiltration	308
Horizontal advance of water in the model when Ida and Webster soils are used as the porous media	308
Theoretical horizontal advance of irrigation water when the infiltration equation is $y = At^{1/2} + Bt$ and the parameters A and B are determined under field conditions	309
Theoretical horizontal advance of irrigation water when the infiltration equation is $y = Kt$, as for sand	312
Discussion	314
Bibliography	316



SUMMARY

Mathematical equations describing the horizontal advance of an irrigation stream on a soil surface are derived and discussed for different types of infiltration equations corresponding to different known field conditions. Complex variable theory is applied to transform certain complicated forms of infiltration equation solutions to algebraic forms. An irrigation model having a visible Plexiglas photographic front was constructed and operated to test the theory and obtain data not covered by the theory. Glass beads or soil aggregates constitute the porous medium; water is used as the seepage fluid. Potassium dichromate dye is injected into the porous medium to trace the direction and velocity of the stream lines when the water moves within the body of the porous medium. The model data are recorded by photography and show a good agreement between theory and experiment for both the calculated position of the "irrigation" front on the porous media and the "wetted" front below the surface. Comparisons were made between experimental data and theory for two slopes of land, for five porous media, for two irrigation rates, and for two surface conditions, rough and smooth. Dimensionless functions are developed to present the model data.

For sandy soils, where capillary effects are negligible, the infiltration equation is of the type

$$y = Kt$$

where

y = the cumulative infiltration in cm^3/cm^2

t = the time in min

K = the Darcy coefficient with dimensions cm/min

Our theory predicts the depth of infiltration of irrigation water and the maximum distance the irrigation water will advance horizontally on the surface of such sandy soils. Dimensionless functions are developed when the infiltration equation is assumed to be

$$y = Et^\alpha$$

where

y and t are as defined before

E = a coefficient with dimensions $(\text{cm}) (\text{min})^{-\alpha}$

α = a dimensionless coefficient

These dimensionless functions predict the position of the advancing water on the soil surface as a function of time and also the cumulative infiltration at each position along the irrigation check.

Another type of infiltration equation is known for certain soils to be

$$y = At^{1/2} + Bt$$

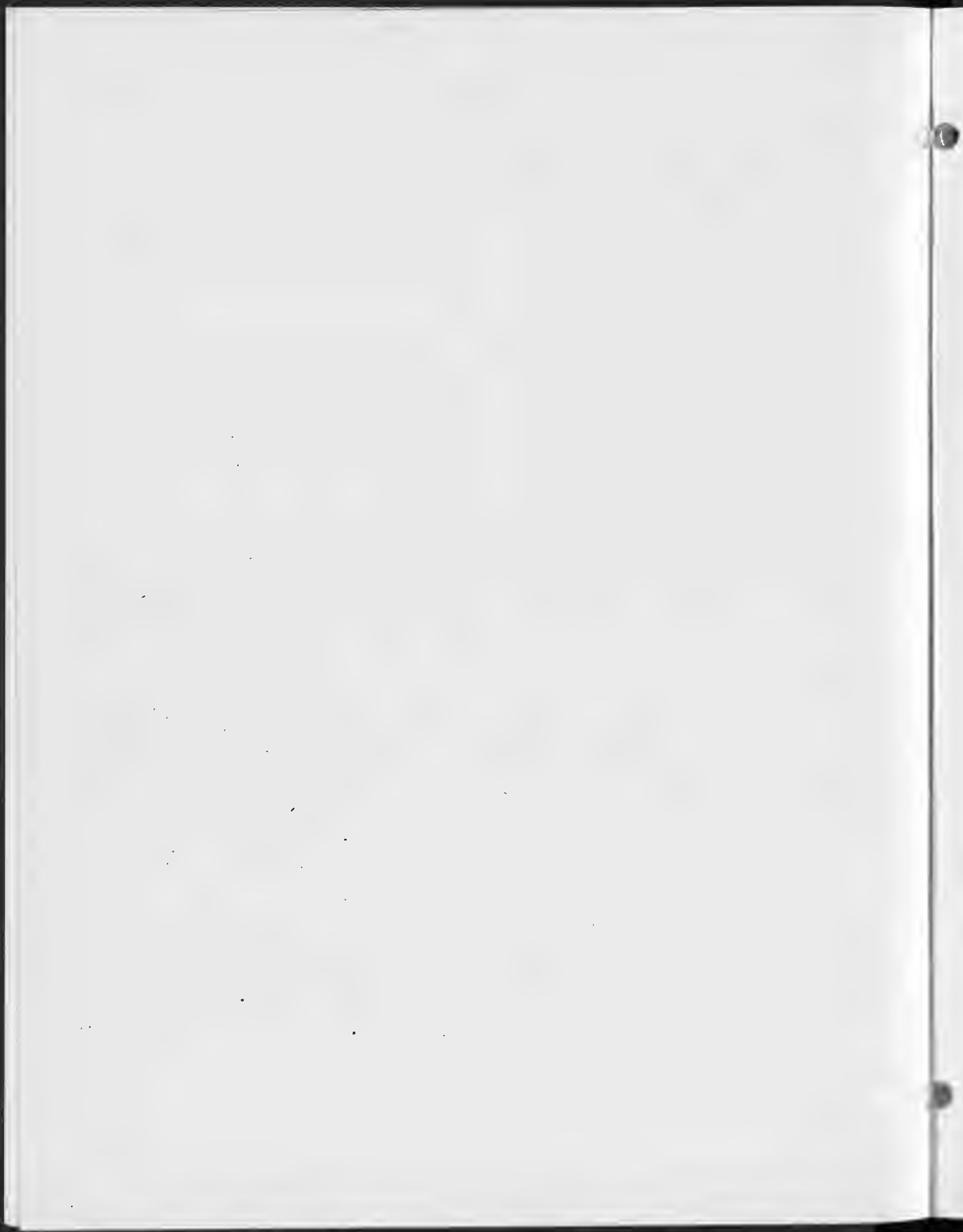
where

y and t are as defined before

A = a coefficient with dimensions $(\text{cm}) (\text{min})^{-1/2}$

B = a coefficient with dimensions $(\text{cm}) (\text{min})^{-1}$

Our theory also predicts the depth of infiltration of irrigation water for such soils.



Advance of Irrigation Water on the Soil Surface in Relation to Soil Infiltration Rate: A Mathematical and Laboratory Model Study¹

by Mohamed Asseed² and Don Kirkham³

The purpose of this study was to determine the rate of horizontal advance of irrigation water as related to the infiltration characteristics of soils. The specific objectives were to: (a) design and operate an irrigation model to determine the horizontal advance of water on the surface for different porous media with different infiltration characteristics and for different conditions of surface slope and roughness, (b) compare mathematical solutions with model data, (c) use dimensionless functions to represent the model data and (d) use various infiltration equations to develop theoretical curves for the horizontal advance of flooding irrigation water on the surface of soil.

THEORY

Derivation of the Irrigation Advance Equation

We are concerned (fig. 1) with the advance of water down an irrigation check (an irrigation check is a confined rectangular area to be irrigated) when a volume of flow V is introduced at its head. The flow equation may then be written as

$$V = Qt_x \quad (1)$$

where

V = volume of water, in cm^3 , that has flowed from the head of the check during the interval $t = 0$ to $t = t_x$

Q = rate of water flow, in cm^3/sec , into the check

t_x = elapsed time, in sec, for the surface water to advance a distance x

Let L be the width of the irrigation check, C the depth of ponded surface water, and y the cumulative infiltration at time t when the irrigation water advances a distance s . Then, by continuity, the total volume of water $V = Qt_x$ above and beneath the soil is

$$Qt_x = L \int_0^x (C + y) ds \quad (2)$$

Let us define t_s as the time for the surface water to

advance a distance s and t_x as the time for the surface water to advance a distance x . Then, the time for water to be available for infiltration at the point D in fig. 1 is $t_x - t_s$. Thus, we see that y in eq. 2 is a function of $(t_x - t_s)$; that is, $y = f(t_x - t_s)$. After introducing this new form of y into eq. 2 and dividing both sides of eq. 2 by L , we obtain

$$\begin{aligned} \frac{Q}{L} t_x &= \int_0^x C ds + \int_0^x f(t_x - t_s) ds \\ &= \int_0^x C ds + \int_0^x f(t_x - t_s) \frac{ds dt_s}{dt_s} \\ &= \int_0^x C ds + \int_0^t f(t_x - t_s) x'(t_s) dt_s \end{aligned} \quad (3)$$

where

the limits 0 and x are changed into the limits 0 and t because:

when $t = 0$, we have $x = 0$

when $t = t$, we have $x = x$

and where we have used the notation

$$x'(t_s) = \frac{ds}{dt_s} \quad (4)$$

If we further introduce a new symbol q , defined by

$$q = Q/L$$

such that q is the amount of water that flows per unit of width of check per unit time, then we may, after dropping the subscript x on t , write eq. 3 in the form

$$qt = Cx + \int_0^t f(t - t_s) x'(t_s) dt_s \quad (5)$$

where $x' = x'(t_s)$; that is, x' is a function of t_s .

Physically we see that x is a monotonic increasing function of t up to some value of t and some value of x (if the irrigation run, as assumed here, is long enough and if the soil absorbs all the applied water).

In deriving eq. 5, it is assumed that the value of C , the depth of ponded surface water, is constant along the irrigation run and is independent of time. An unpublished study by Farrell (see Philip and Farrell, 1964) suggests that C is, indeed, very nearly independent of time under a wide range of conditions. Evidently, C will depend on q and on the surface slope and hydraulic roughness of the irrigation check.

¹ Projects 998 and 1653, Iowa Agriculture and Home Economics Experiment Station. This research was supported in part with funds provided by the Department of the Interior, Office of Water Resources Research, under P.L. 88-379. The authors are greatly indebted to Mr. Sadik Toksoz, formerly chief, Groundwater and Irrigation Branch, Harza Engineering Company International, Lahore, West Pakistan, and presently research associate, Iowa State University, for a thorough review and many useful suggestions.

² Formerly research assistant, Department of Agronomy, Iowa State University. Presently a Post doctoral Fellow, Department of Agronomy, Purdue University.

³ Professor of soils and physics, Iowa State University, Ames.

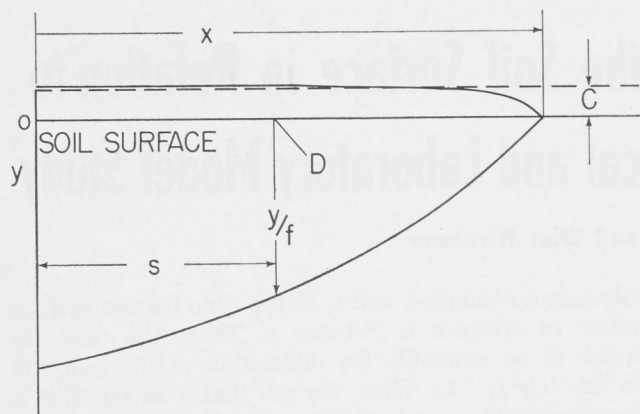


Fig. 1. Depth of surface water that has entered vertically at point D into a unit area of soil, resulting in a depth of penetration y/f with f being constant porosity, when the point D is at a distance s from the position O of irrigation water application and when the surface water has advanced a distance x . The value of y is a function of $t_x - t_s$, where t_x is the time for the surface water to advance the distance x and t_s is the time for the surface water to advance a distance s . C is the average surface depth of irrigation water.

Thus, the theory takes into account the surface slope and hydraulic roughness of the irrigation check through the parameter C . The hydraulic roughness, by itself, and its effects on the overland flow are complex and very difficult to evaluate. The roughness coefficient varies greatly with the depth of flow. Flows at shallow depths encounter a maximum resistance because the vegetation is upright in the flow. As the depth of flow increases, the depressions on the soil surface are filled, and more and more vegetation is submerged, with an accompanying decrease in flow resistance. The surface slope also influences the resistance to flow. Decreasing resistance obviously results from higher flow velocities on steeper slopes.

We shall now apply eq. 5 to some special cases.

Solution for the Infiltration Case $y = Kt$

The cumulative infiltration equation $y = Kt$ describes the infiltration of irrigation water in a sandy soil (seen immediately by applying Darcy's law to downward movement in a porous medium having negligible capillary forces). Using $y = Kt$ in eq. 5, we find

$$qt = Cx(t) + K \int_0^t (t - t_s) x'(t_s) dt_s \quad (6)$$

Differentiation of eq. 6 with respect to t gives, after use of eq. 4, the expressions

$$q = C \frac{dx}{dt} + K \int_0^t x'(t_s) dt_s + [K x'(t_s)] [t - t_s]$$

where $t - t = 0$

$$\begin{aligned} q &= C \frac{dx}{dt} + K \int_0^t x'(t_s) dt_s \\ &= C \frac{dx}{dt} + Kx(t) - Kx(0) \end{aligned}$$

The last expression yields

$$q = C \frac{dx}{dt} + Kx(t) \quad (7)$$

because, physically, at zero time we have $x(0) = 0$.

Eq. 7 is an ordinary linear differential equation, which can be written

$$\frac{dx}{dt} + \frac{K}{C} x(t) = \frac{q}{C} \quad (8)$$

An integration factor for eq. 8 is of the form

$$\exp \int \frac{K}{C} dt = \exp \frac{K}{C} t$$

If we multiply eq. 8 by this integration factor, we find

$$\begin{aligned} (\exp \frac{K}{C} t) \frac{dx}{dt} + \frac{K}{C} (\exp \frac{K}{C} t) x(t) \\ = \frac{q}{C} \exp \frac{K}{C} t \end{aligned} \quad (9)$$

which gives

$$\frac{d}{dt} [x(t) \exp \frac{K}{C} t] = \frac{q}{C} \exp \frac{K}{C} t \quad (10)$$

Integration of eq. 10 gives

$$x(t) \exp \frac{K}{C} t = \frac{q}{K} \exp \frac{K}{C} t + C' \quad (11)$$

where C' is a constant of integration.

When $t = 0$, we have $x = 0$. Therefore, we find

$$C' = -\frac{q}{K}$$

and eq. 11 yields the solution

$$x(t) = \frac{q}{K} [1 - \exp(-\frac{K}{C} t)] \quad (12)$$

Eq. 12 gives, when t approaches infinity, the result

$$\lim_{t \rightarrow \infty} x(t) = \frac{q}{K} \quad (13)$$

which corresponds to Darcy's law being applied to surface inflow into an infinitely deep homogeneous saturated soil over the whole distance x . For this last situation, K in eq. 13 is the Darcy law K for the soil and has dimensions length over time, or volume per unit area per unit time.

Eq. 13 shows that, when we apply a constant amount of irrigation water q at the head of the irrigation check in sandy soils, the maximum distance that water will advance horizontally on the surface is q/K , where K is the slope of the line when the cumulative infiltration $y(\text{cm}^3/\text{cm}^2)$ is plotted versus time and q is the amount of applied irrigation water per unit width of the field per unit time.

Solution for the Infiltration Case $y = Et^\alpha$

Let E be a soil water entry coefficient and α a dimensionless parameter $0 < \alpha < 1$; then the solution of eq. 5, when the cumulative infiltration is given by the equation $y = Et^\alpha$, is that found by Philip and Farrell (1964), and we will discuss the validity of the solution. Philip and Farrell's solution, in terms of an infinite series, is

$$\frac{x}{q} = \frac{t}{C} \sum_{n=0}^{\infty} \frac{\{(-Et^\alpha/C)[\Gamma(1+\alpha)]\}^n}{\Gamma(2+na)} \quad (14)$$

where, Γ represents the Gamma function and other symbols are as before.

Eq. 14 converges absolutely according to the ratio test (see Fulks, 1962). If we apply the ratio test, we will have

$$\begin{aligned} \frac{Et^\alpha \cdot \Gamma(1+\alpha) \cdot \Gamma(2+na)}{C \Gamma[2+(n+1)\alpha]} &= \\ \frac{E \cdot \Gamma(1+\alpha) \cdot t^\alpha \Gamma(2+na)}{C \Gamma(2+na+\alpha)} &= \frac{E \cdot \Gamma(1+\alpha) \cdot t^\alpha}{C} \\ \cdot \frac{1}{(2+na)^\alpha} \cdot \frac{(2+na)^\alpha \Gamma(2+na)}{\Gamma(2+na+\alpha)} & \quad (15) \end{aligned}$$

But we have

$$\lim_{n \rightarrow \infty} \frac{1}{(2+na)^\alpha} = 0$$

and, proved in Hille (1959, p. 238, eq. 8.8.38), we have the relation

$$\lim_{n \rightarrow \infty} \frac{(2+na)^\alpha \Gamma(2+na)}{\Gamma(2+na+\alpha)} = 1$$

so for any value of t , each equality in expression 15 $\rightarrow 0$ as $n \rightarrow \infty$, and the right side of eq. 14 must converge for all t . But unfortunately, the computer program does not yield values for eq. 14 beyond a specific value of t . Wilke and Smerdon (1965) also found that the computer program would not give appropriate values for eq. 14 for large values of Et^α/C . In the range where the computer program failed, Smerdon and Wilke assumed a straight line relation; this has been criticized by Chen (1966). Our experimental work (see later) shows that a straight line relation holds for a large range of values of Et^α/C .

In eq. 14, if we rearrange the equation as

$$\frac{Cx}{qt} = \sum_{n=0}^{\infty} \frac{[(-Et^\alpha/C)\Gamma(1+\alpha)]^n}{\Gamma(2+na)} \quad (16)$$

there appear dimensionless quantities Cx/qt and Et^α/C , which we may plot against each other. We can do this even for large values of t if we use experi-

mental values of x , q , t , E , C and α . We can use our laboratory data to plot Cx/qt versus Et^α/C and then use these graphs (see Grover and Kirkham, 1964) to predict irrigation advance x and infiltration depth y . We shall see later that, within experimental error, a graph qt/xC versus Et^α/C is linear over the range of values and conditions we used (but the straight line does not go through the origin). Equations of the form $qt/Cx = a + bEt^\alpha/C$ were derived by using our model experimental data and will be discussed in "Results and Discussion."

Solution for the Infiltration Case $y = At^{1/2} + Bt$

The infiltration equation $y = At^{1/2} + Bt$ was derived theoretically by Philip (1957a, 1957b, 1957c, 1958a and 1958b). Philip's theory is applicable to conditions where t is not too large. The first term, $At^{1/2}$, on the right-hand side of the infiltration equation derived by Philip represents the contribution arising from capillarity, and the second term, Bt , consists essentially of the contribution arising from gravity. The equation $y = At^{1/2} + Bt$ was used by Philip and Farrell (1964) to derive an irrigation infiltration equation. Philip and Farrell's solution is not suitable for numerical computation, so we obtain another solution. We follow Philip and Farrell up to eq. 31, filling in missing steps.

We use, following Churchill (1941, 1958, 1960) and Holl et al. (1959), symbols L , F , f , s and t for Laplace transforms (these symbols having no relation to preceding symbols) as follows:

$$L\{F\} = \int_0^{\infty} e^{-st} F(t) dt = f(s) \quad (17)$$

$$F(t) = L^{-1}\{f(s)\} \quad (18)$$

Applying the convolution theorem (Holl et al., 1959, pp. 43-49) and taking the Laplace transformation of eq. 5 we get (with q , s , x , x' and y as in eq. 5) the expression

$$\begin{aligned} q/s^2 &= CL\{x\} + L\{x'\} L\{y\} \\ &= CL\{x\} + [sL\{x\} - x(0)]L\{y\} \\ &= CL\{x\} + sL\{x\} L\{y\} \end{aligned} \quad (19)$$

Since we have $x(0) = 0$, we see that eq. 19 reduces to

$$\frac{L\{x\}}{q} = \frac{1}{s^3 L\{y\} + C s^2} \quad (20)$$

in which we need a value of $L\{y\}$ where we now have, by hypothesis, the expression

$$y = At^{1/2} + Bt$$

From a handbook of Laplace transforms (as Holl et al., 1959, p. 148, third entry with $\alpha = 1$ and $\alpha = 1/2$, we find

$$\begin{aligned} L\{y\} &= AL\{t^{1/2}\} + BL(t) \\ &= A \frac{\Gamma(1/2 + 1)}{s^{1/2 + 1}} + B \frac{1}{s^2} \end{aligned} \quad (21)$$

But we have the relations

$$\Gamma(x + 1) = x\Gamma(x), \quad \Gamma(1/2) = \pi^{1/2}$$

so that eq. 21 becomes

$$L\{y\} = \frac{A\pi^{1/2}}{2s^{3/2}} + B \frac{1}{s^2} \quad (22)$$

Combining eqs. 20 and 22, we have

$$\frac{L\{x\}}{q} = \frac{1}{s^3 [\frac{1}{2}\pi^{1/2} A s^{-3/2} + B s^{-2}] + C s^2} \quad (23)$$

or we have

$$\frac{x}{q} = L^{-1} \left\{ \frac{1}{C s^2 + A \frac{\pi^{1/2}}{2} s^{3/2} + B s} \right\} \quad (24)$$

To put eq. 24 in an easy form for getting the inverse of the Laplace transform, two quantities are introduced

$$\gamma = \frac{1}{4C} [\pi^{1/2} A + (\pi A^2 - 16 BC)^{1/2}] \quad (25)$$

$$\beta = \frac{1}{4C} [\pi^{1/2} A - (\pi A^2 - 16 BC)^{1/2}] \quad (26)$$

Substituting γ and β in eq. 24, we have

$$\begin{aligned} \frac{x}{q} &= L^{-1} \left\{ \frac{1}{Cs[s + s^{1/2}(\gamma + \beta) + \gamma\beta]} \right\} \\ &= L^{-1} \left\{ \frac{1}{Cs[s + s^{1/2}\gamma + s^{1/2}\beta + \gamma\beta]} \right\} \end{aligned} \quad (27)$$

We now multiply the right side of eq. 27 by unity in the form

$$\frac{\gamma - \beta}{\gamma - \beta}$$

to obtain

$$\begin{aligned} \frac{x}{q} &= L^{-1} \left\{ \frac{\gamma - \beta}{Cs[\gamma - \beta][s + s^{1/2}\gamma + s^{1/2}\beta + \gamma\beta]} \right\} \\ &= L^{-1} \left\{ \frac{\gamma - \beta + s^{1/2} - s^{1/2}}{Cs[\gamma - \beta][s + s^{1/2}\gamma + s^{1/2}\beta + \gamma\beta]} \right\} \\ &= L^{-1} \left\{ \frac{[s^{1/2} + \gamma] - [s^{1/2} + \beta]}{Cs(\gamma - \beta)[s^{1/2} + \gamma][s^{1/2} + \beta]} \right\} \end{aligned}$$

$$\frac{1}{C(\gamma - \beta)} L^{-1} \left\{ \frac{1}{s(s^{1/2} + \beta)} - \frac{1}{s(s^{1/2} + \gamma)} \right\} \quad (28)$$

We need to recall the definitions of the error function of $z (= \operatorname{erf} z)$ and of the complementary error function of $z (= \operatorname{erfc} z)$. These definitions are (see Abramowitz and Stegun, 1964)

$$\operatorname{erf} z = \frac{1}{2\pi} \int_{t=0}^{t=z} \exp - t^2 dt \quad (28a)$$

$$\operatorname{erfc} z = \frac{1}{2\pi} \int_{t=z}^{\infty} \exp - t^2 dt \quad (28b)$$

which gives because of

$$\int_0^{\infty} (\exp - t^2) dt = 2\pi$$

the relation (and hence the name, "complementary error function")

$$\operatorname{erfc} z = 1 - \operatorname{erf} z$$

We now can get the inverse of the Laplace transform of eq. 28, From Hodgman et al. (1957-1958, p. 290, eq. 86), we have

$$\begin{aligned} L^{-1} \left\{ \frac{a \exp(-hs^{1/2})}{s(s^{1/2} + a)} \right\} &= \\ &= -(\exp ah) (\exp a^2 t) \operatorname{erfc} (at^{1/2} + \frac{h}{2t^{1/2}}) \\ &\quad + \operatorname{erfc} (\frac{h}{2t^{1/2}}) \end{aligned} \quad (29)$$

In our case, $h = 0$, so we have

$$\begin{aligned} L^{-1} \left\{ \frac{a}{s(s^{1/2} + a)} \right\} &= -(\exp a^2 t) \operatorname{erfc} (at^{1/2} + 0) + 1 \\ &= 1 - (\exp a^2 t) (\operatorname{erfc} at^{1/2}) \end{aligned} \quad (30)$$

Eq. 28 can be written as

$$\frac{x}{q} = \frac{1}{(\gamma - \beta)C} L^{-1} \left\{ \frac{1}{\beta} \frac{\beta}{s(s^{1/2} + \beta)} - \frac{1}{\gamma} \frac{\gamma}{s(s^{1/2} + \gamma)} \right\} \quad (31)$$

Now we can take the inverse of eq. 31, so

$$\begin{aligned} \frac{x}{q} &= \frac{1}{(\gamma - \beta)C} \left\{ \frac{1}{\beta} [1 - \exp \beta^2 t (\operatorname{erfc} \beta t^{1/2})] \right. \\ &\quad \left. - \frac{1}{\gamma} [1 - \exp \gamma^2 t (\operatorname{erfc} \gamma t^{1/2})] \right\} \end{aligned} \quad (32)$$

Eq. 32 is the solution for eq. 23 when γ and β are both real numbers, but when $C > \pi A^2 / (16B)$, both γ and β will be complex and will take the forms

$$\gamma = \frac{1}{4C} [\pi^{1/2} A + i(16 BC - \pi A^2)^{1/2}] \quad (33)$$

$$\beta = \frac{1}{4C} [\pi^{1/2} A - i(16 BC - \pi A^2)^{1/2}] \quad (34)$$

But from complex variables (Churchill, 1960), if we define $W(u)$ and $W(u)^*$ by the expressions (in which $i = (-1)^{1/2}$)

$$W(u) = u(x,y) + iu(x,y)$$

$$W(u)^* = u(x,y) - iu(x,y)$$

then we see that $W(u)^*$ signifies the conjugate of $W(u)$, and hence, eq. 33 is the conjugate of eq. 34. That is, we have the relation $\gamma = \beta^*$. Our solution for $C > \pi A^2/(16B)$ now may be written as

$$\frac{x}{q} = \frac{1}{\beta^* - \beta} \left\{ \frac{1}{C\beta} [1 - \exp \beta^2 t (\operatorname{erfc} \beta t^{1/2})] - \frac{1}{C\beta^*} [1 - \exp \beta^* t (\operatorname{erfc} \beta^* t^{1/2})] \right\} \quad (35)$$

Eq. 35 is complicated and not suitable for numerical work. By using values of A and B , obtained from field infiltration studies, we found that the condition $C > \pi A^2/(16B)$ that governs eq. 35 is the condition most often encountered in the field. Therefore, a practical solution to replace eq. 35 is needed.

We have, by definition

$$\beta^* = u + iv \quad (36)$$

$$\beta = u - iv \quad (37)$$

where $u =$ the real part of β^* , and $v =$ the imaginary part. In keeping with eq. 36 and 37, we let z and g be defined by the equations (the second equation in each line being a consequence of the first)

$$z = i\beta t^{1/2} = (iu + v)t^{1/2}, \quad -iz = \beta t^{1/2} \quad (38)$$

$$g = i\beta^* t^{1/2} = (iu - v)t^{1/2}, \quad -ig = \beta^* t^{1/2} \quad (39)$$

$$z^2 = (i\beta t^{1/2})^2 = -\beta^2 t, \quad -z^2 = \beta^2 t \quad (40)$$

$$g^2 = (i\beta^* t^{1/2})^2 = -\beta^{*2} t, \quad -g^2 = \beta^{*2} t \quad (41)$$

From eqs. 38-41, we may write two identities

$$\begin{aligned} & [1 - (\exp \beta^2 t) (\operatorname{erfc} \beta t^{1/2})] \\ & = [1 - (\exp - z^2) (\operatorname{erfc} - iz)] \end{aligned} \quad (42)$$

$$\begin{aligned} & [1 - (\exp \beta^{*2} t) (\operatorname{erfc} \beta^* t^{1/2})] \\ & = [1 - (\exp - g^2) (\operatorname{erfc} - ig)] \end{aligned} \quad (43)$$

We now substitute eqs. 42 and 43 in eq. 35 and find

$$\begin{aligned} \frac{x}{q} &= \frac{1}{(\beta^* - \beta)} \left\{ \frac{1}{\beta C} [1 - (\exp - z^2) (\operatorname{erfc} - iz)] \right. \\ &\quad \left. - \frac{1}{\beta^* C} [1 - (\exp - g^2) (\operatorname{erfc} - ig)] \right\} \end{aligned} \quad (44)$$

If we now define $w(z)$ and $w(g)$ by

$$w(z) = (\exp - z^2) (\operatorname{erfc} - iz) \quad (45)$$

$$w(g) = (\exp - g^2) (\operatorname{erfc} - ig) \quad (46)$$

eq. 44 will take the form

$$\begin{aligned} \frac{x}{q} &= \frac{1}{\beta^* - \beta} \left[\frac{1 - w(z)}{C\beta} - \frac{1 - w(g)}{C\beta^*} \right] \\ &= \frac{1}{(\beta^* - \beta)C} \left[\frac{\beta^*(1 - w(z))}{\beta^*\beta} - \frac{\beta(1 - w(g))}{\beta\beta^*} \right] \end{aligned} \quad (47)$$

But we have

$$\begin{aligned} \beta^*\beta &= (u + iv)(u - iv) = u^2 - iuv + iuv - i^2v^2 \\ &= u^2 + v^2 \end{aligned} \quad (48)$$

$$\beta^* - \beta = u + iv - u + iv = 2iv \quad (49)$$

We put eqs. 48 and 49 in eq. 44 and find

$$\begin{aligned} \frac{x}{q} &= \frac{1}{(2iv)C} \left\{ \frac{[u + iv][1 - w(z)]}{u^2 + v^2} - \frac{[u - iv][1 - w(g)]}{u^2 + v^2} \right\} \\ &= \frac{1}{(2iv)C} \end{aligned} \quad (50)$$

$$\left\{ \frac{[u + iv][1 - R(w_z) - iI(w_z)] - [u - iv][1 - R(w_g) - iI(w_g)]}{u^2 + v^2} \right\}$$

where we have

$R(w_z) =$ real part of the function $w(z)$

$I(w_z) =$ imaginary part of the function $w(z)$

$R(w_g) =$ the real part of the function $w(g)$

$I(w_g) =$ the imaginary part of the function $w(g)$

To establish the relation between $R(w_z)$, $R(w_g)$, $I(w_z)$ and $I(w_g)$, we proceed by using eqs. 38, 39, 45, 46 and 28b to find

$$\begin{aligned} w(z) &= w[t^{1/2}(v - iu)] \\ &= \left\{ \exp[-t(v + iu)^2] \right\} \left\{ \left(\frac{2}{\pi^{1/2}} \right) \int_0^\alpha \frac{(\exp - t^2) dt}{(u + iv)t^{1/2}} \right\} \end{aligned} \quad (51)$$

Similarly, we have

$$\begin{aligned} w(g) &= w[t^{1/2}(-v + iu)] \\ &= \left\{ \exp[-t(-v + iu)^2] \right\} \left\{ \left(\frac{2}{\pi^{1/2}} \right) \int_0^\infty \frac{(\exp - t^2) dt}{(u + iv)t^{1/2}} \right\} \end{aligned} \quad (52)$$

But we have

$$\exp[-t(-v + iu)^2] = \exp[-t(v^2 - u^2 - ziuiv)] \quad (53)$$

$$\exp[-t(v + iu)^2] = \exp[-t(v^2 - u^2 + ziuiv)] \quad (54)$$

so that we have

$$\begin{aligned} \exp[-t(-v + iu)^2] &= \\ &\quad \text{the conjugate of } \exp[-t(v + iu)^2] \end{aligned} \quad (55)$$

Also, we have

$$\frac{2}{\pi^{1/2}} \int_0^{\infty} \frac{(\exp - t^2) dt}{(u + iv) t^{1/2}} \quad (56)$$

$$= \text{the conjugate of } \frac{2}{\pi^{1/2}} \int_0^{\infty} \frac{(\exp - t^2) dt}{(u - iv) t^{1/2}}$$

Comparing eqs. 55 and 56 with eqs. 51 and 52, we find, by using the star convention of eqs. 36 and 37, the result

$$[w(g)] = [w(z)]^* \quad (57)$$

or we find

$$R(w_g) + i I(w_g) = R(w_z) - i I(w_z) \quad (58)$$

which gives, by equating coefficients of reals and imaginaries, the results

$$R(w_g) = R(w_z) \quad (59)$$

$$I(w_g) = -I(w_z) \quad (60)$$

Applying eqs. 59 and 60 to eq. 50 we find

$$\frac{x}{q} = \frac{1}{(2iv)C} \left[\frac{2iv - 2iuI(w_z) - 2ivR(w_z)}{u^2 + v^2} \right] \quad (61)$$

so our final algebraic equation is

$$\frac{x}{q} = \left\{ \frac{v[1 - R(w_z)] - u I(w_z)}{C \cdot v(u^2 + v^2)} \right\} \quad (62)$$

where we have

$$u = R(\beta^*) = \frac{\pi^{1/2} A}{4C}$$

$$v = I(\beta^*) = \frac{(16BC - \pi A^2)^{1/2}}{4C}$$

and where $w(z) = (\exp - z^2) [\operatorname{erfc}(iz)]$ is a function that is tabulated in Faddeyeva and Terentev (1961). To match the notation of Faddeyeva and Terentev (1961) with the notation used here we have

$$X_F [\text{in Faddeyeva and Terentev}] = \frac{t^{1/2} (16BC - \pi A^2)^{1/2}}{4C}$$

$$Y_F [\text{in Faddeyeva and Terentev}] = \frac{t^{1/2} \pi^{1/2} A}{4C}$$

Thus, the values of X_F and Y_F are calculated for each given time t from the constants A and B , which are given in the cumulative infiltration equation. After we have calculated X_F and Y_F , we find values of $R(w_z)$ and $I(w_z)$ from the tables of Faddeyeva and Terentev. Then, $\frac{x}{q}$ can easily be obtained by eq. 62.

EXPERIMENT

The Irrigation Model

Fig. 2 illustrates a front elevation of the model and

gives model dimensions. The model was constructed from Plexiglas, a transparent and craze-resistant plastic material. The back and edges of the model were painted with a flat-finish black paint to produce a dark background. A model thickness of 1.9 cm was obtained by using triple thickness spacers of Plexiglas. The left end (see fig. 2) of the model was shortened 1 cm to allow an overflow from a simulated irrigation head-ditch, 5 cm deep and 4 cm wide, affixed to the side of the model. The ditch was used to supply the model with a constant feeding quantity of water. Ten small holes for dye injection were drilled in the front of the model. The dye used was potassium dichromate (Kirkham, 1940). It colored the streamlines that developed when the water penetrated the porous medium. At the back of the model, five rows of holes were drilled for sampling for moisture determination. This set of holes, plus another set of holes in the bottom of the model, allowed escape of air during infiltration.

To get soil moisture samples at the same instant from the columns of vertical holes at the back of the model, five sampler devices were constructed from Plexiglas and brass tubes. Each of these five samplers fitted a set of four vertical holes, and 20 moisture samples were taken simultaneously at the end of an irrigation test.

The Water-Feeding System

A system was constructed to provide simulated irrigation water at a constant rate to the head ditch of the model. The principal item of the system was a cylinder constructed from Plexiglas. Two holes were drilled at the bottom of the cylinder, and two capillary tubes were affixed by rubber stoppers. Capillary tubes of different radii were used for different runs to obtain different rates of water application. The head difference of water across the capillary tubes could also be changed. The head of water in the cylinder was maintained constant during a run by a "Mariotte" flask device.

Porous Media Used in the Model and their Infiltration Characteristics

Porous media of different infiltration characteristics were used in the model. Three sizes of glass beads

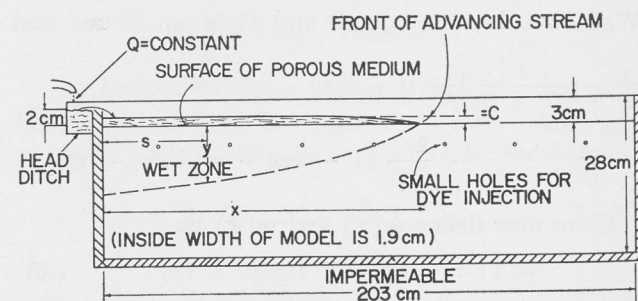


Fig. 2. Schematic diagram of the model.

with average diameters of 28, 50 and 100 μ were used. Aggregates of Ida silt loam and Webster clay loam were also used in separate runs. The soil aggregates were of size < 2 mm.

Cumulative infiltration data for each porous

medium were obtained by isolating a section from the model, packing this section with glass beads or soil, ponding a layer of water on the surface and measuring with time the volume of applied water that was absorbed vertically by the section of porous medium. The infiltration data were obtained in this way to characterize the porous medium in the model for use when later "irrigation" runs were conducted.

Figs. 3 and 4 show the infiltration data for glass beads and for soil aggregates. For glass beads, the infiltration data fitted the equation $y = Et^\alpha$, where y is the cumulative infiltration in cm^3/cm^2 , t is time in minutes and E and α are constants. For the aggregates of Ida and of Webster soil, we see that the infiltration data fitted Philip's infiltration equation, $y = At^{1/2} + Bt$, where y is the cumulative infiltration in cm^3/cm^2 , t is time in minutes, and A and B are constants.

The model experiment was carried out in a constant-temperature room, where the temperature, 25°C , was controlled within $\pm 1^\circ\text{C}$. Thus, the fluid char-

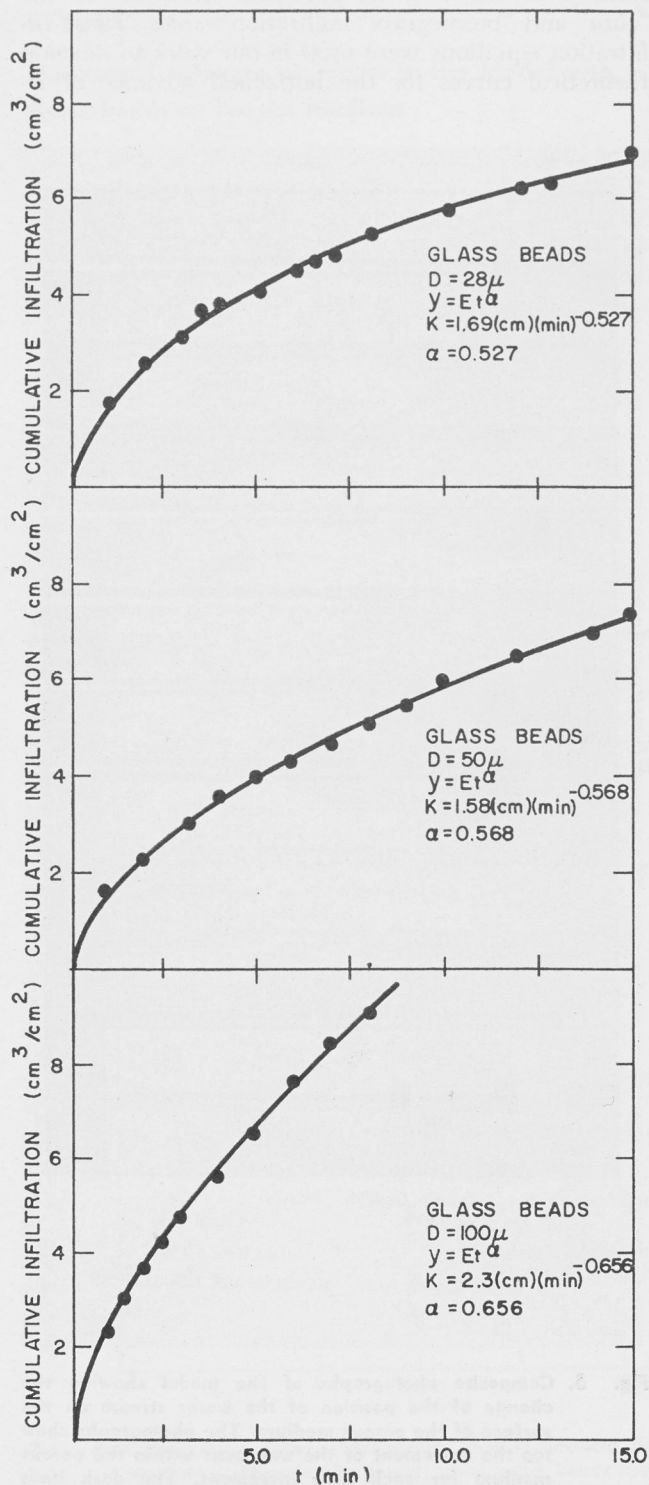


Fig. 3. Cumulative infiltration for initially air-dry glass beads.

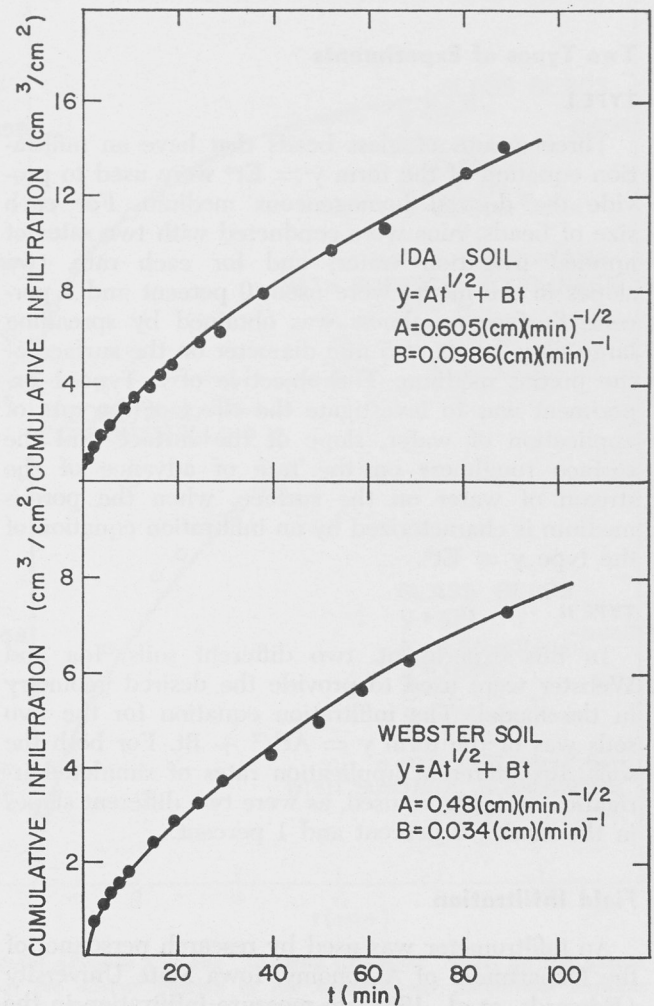


Fig. 4. Cumulative infiltration for initially air-dry Ida and Webster soil.

acteristics, viscosity and mass density would all have the same effect for all the experimental runs.

The glass beads reflect light when surrounded by air, but when surrounded by water, light is transmitted. Thus, by using a black background in the model, we could record by photography the advance of irrigation water on and into the porous medium.

Experimental Procedure

During operation, the model was packed with beads or soil to provide the desired geometry. The surface of the porous medium in the model was leveled. Crystals of potassium dichromate were placed at different positions to show the velocity and direction of streamlines. The feeding system was calibrated to give the required rate of simulated irrigation water for each run. Photographs were taken at several time intervals as the water advanced horizontally on the surface of the porous medium. A clock running counterclockwise was mounted with the model to show the lapsed time between photographs.

Two Types of Experiments

TYPE I

Three groups of glass beads that have an infiltration equation of the form $y = Et^a$ were used to provide the desired homogeneous medium. For each size of beads, runs were conducted with two rates of applied irrigation water; and for each rate, two slopes in the model were used, 0 percent and 1 percent. Surface roughness was obtained by spreading large glass beads of 5 mm diameter on the surface of the porous medium. The objective of a Type 1 experiment was to investigate the effect of the rate of application of water, slope of the surface and the surface roughness on the rate of advance of the stream of water on the surface, when the porous medium is characterized by an infiltration equation of the type $y = Et^a$.

TYPE II

In this experiment, two different soils, Ida and Webster were used to provide the desired geometry in the model. The infiltration equation for the two soils was of the form $y = At^{1/2} + Bt$. For both the soils, two different application rates of simulated irrigation water were used, as were two different slopes in the model, 0 percent and 1 percent.

Field Infiltration

An infiltrometer was used by research personnel of the Department of Agronomy, Iowa State University (Edwards, et al., 1964) to measure infiltration in the field for three Iowa soils: Ida silt loam, Moody silt loam and Grundy silt loam. Within each soil type,

measurements were made on a bare surface representing a newly prepared corn seedbed and on a well-established bromegrass sod. These two surface conditions are referred to in subsequent figures as "corn" and "bromegrass." The infiltration equation of the form $y = At^{1/2} + Bt$ gave the "best fit" to the "corn" and "bromegrass" infiltration values. These infiltration equations were used in our work to develop theoretical curves for the horizontal advance of ir-

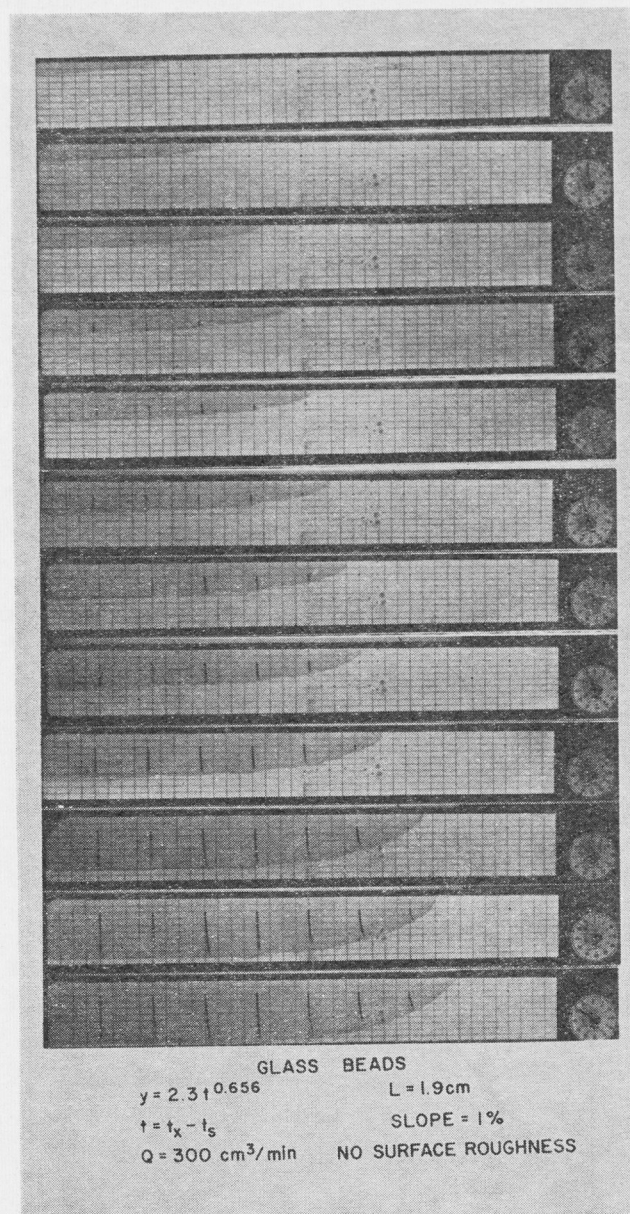


Fig. 5. Composite photographs of the model showing the change of the position of the water stream on the surface of the porous medium. The photographs show too the movement of the wet front within the porous medium for each time increment. The dark lines are the stream lines, colored with potassium dichromate. The description of conditions is shown with the photographs. The clock runs counterclockwise.

rigation water of different rates for the field conditions indicated by the equations. The curves were developed (different values of A and B were found) for the different soil types and for different antecedent moisture contents.

RESULTS

Horizontal Advance of Water in the Model with Glass Beads as Porous Medium

The sets of photographs of the (model) advancing water on the surface and within the porous medium are the raw data for the results; fig. 5 is a sample set. From the sets of photographs, graphs of the distance of horizontal advance of water on the surface of beads in the model have been plotted versus time. The zero

time was the instant the water was applied to the inflow end of the surface of the beads.

The dark gray streamlines of potassium dichromate in fig. 5 show that the movement of water in the porous medium is in the vertical direction at early times during the run, but at later times, the direction of the streamlines deviates from the vertical and tends to move toward the direction of the moving water on the surface. This was expected since there is a hydraulic gradient both in the vertical and horizontal directions within the body of the porous medium. Figs. 6 to 8 give comparisons of the experimental and calculated horizontal distance of advance x of the water stream on the surface of the porous medium in the model. Parts of the calculated curves of figs. 6 to 8 are solid lines. These solid line portions correspond to the curve segments for which the com-

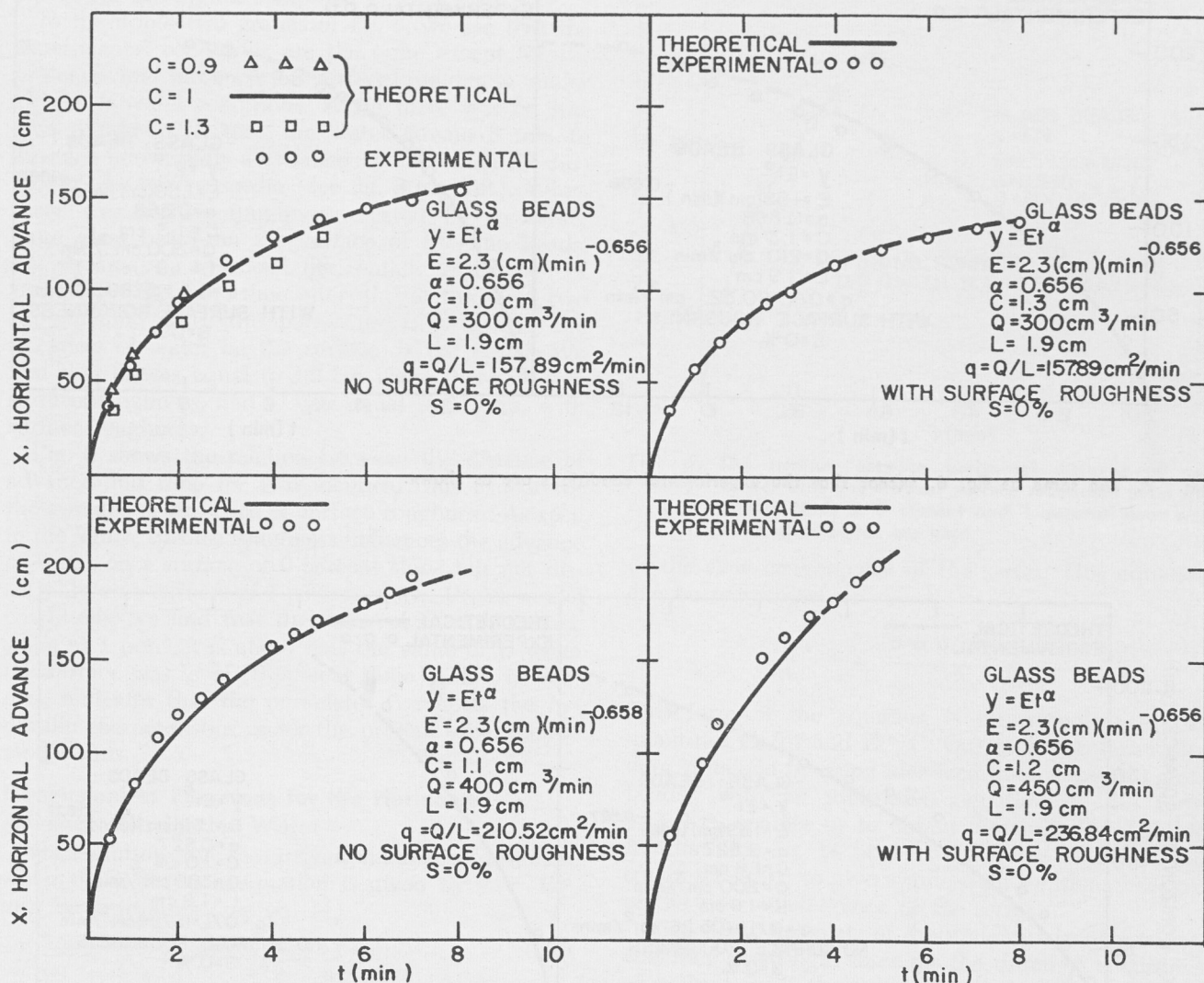


Fig. 6. Comparison of the experimental and theoretical distance of advance x of the "flooding irrigation" water on the porous medium surface in the model, when glass beads are used; the dashed portion of the curve is not theoretical because the computer does not yield a practical value for eq. 14 for values of t in the dashed region. The value of C is averaged from individual values of C for each distance x where plotted. Theoretical curves for $C = 0.9$ and for $C = 1.3$ are shown for comparison.

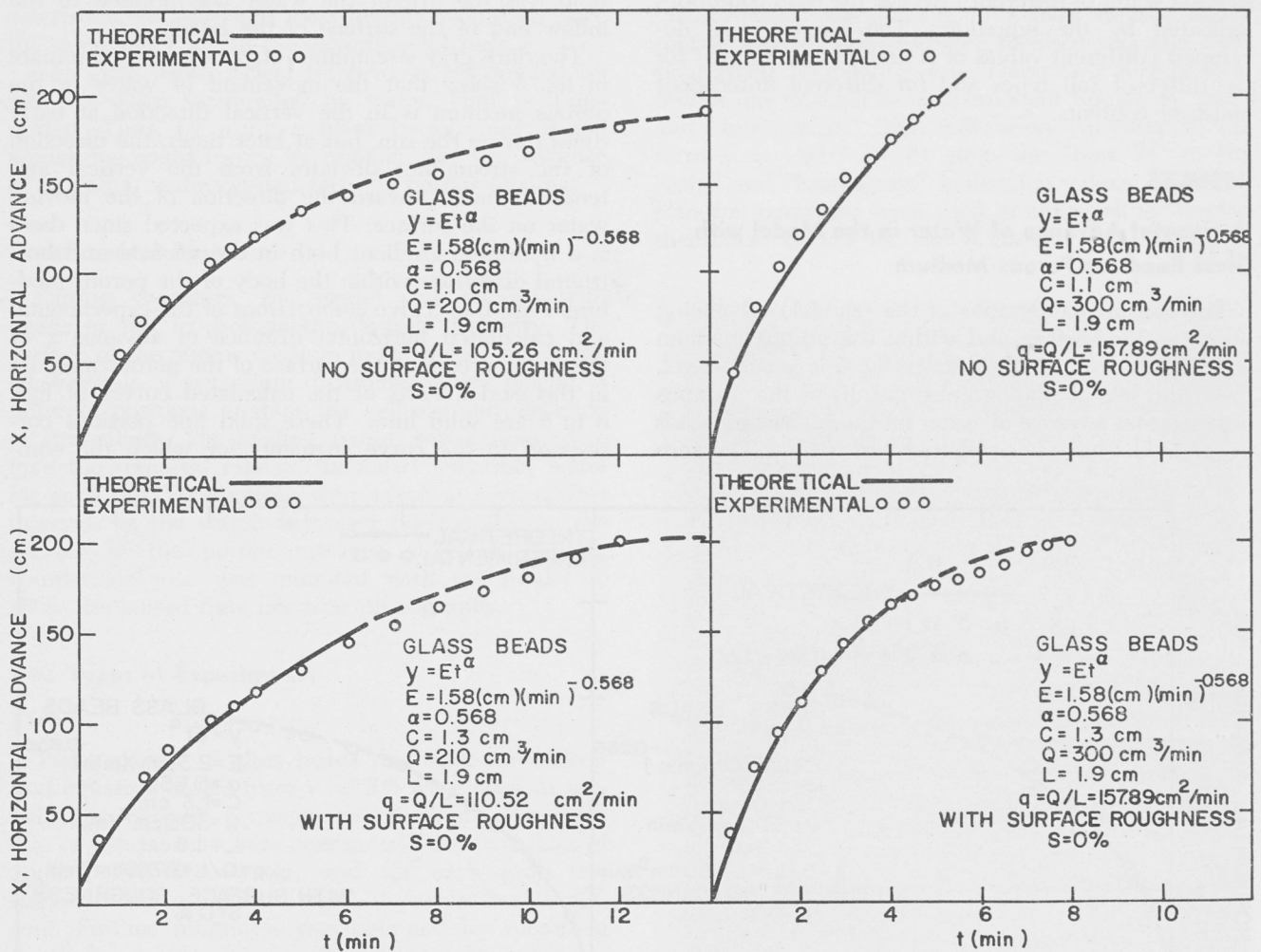


Fig. 7. The same as fig. 6, except that the experimental conditions are as shown.

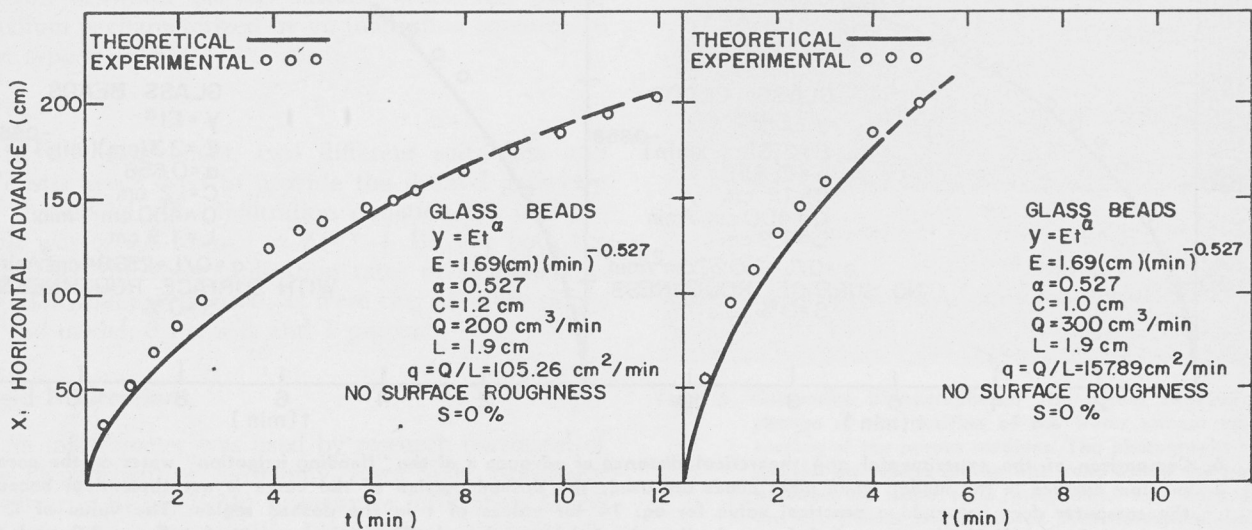


Fig. 8. The same as fig. 6, except that the experimental conditions are as shown.

puter gave values for eq. 14. The experimental points fit these segments. The dashed parts of the curves were drawn by extrapolation to fit the experimental data. Values on the extrapolated parts of our curves were not obtainable by the digital computer because the computations were then beyond the capacity of our program.

Eq. 14 was used in calculating the solid lines of the curves of figs. 6 to 8. The controlling factor for the computer program appears to be the term Et^α/C of the eq. 14. We observe from the top left graph of fig. 6 that the value $x = 143$ cm corresponding to $t = 7$ min is in the dashed, extrapolated portion of the curve. Therefore, the value $Et^\alpha/C = 8.264$ also corresponds to the dashed, extrapolated (not to the solid, computed) portion of the curves. Hence, $Et^\alpha/C = 8.264$ is not an appropriate value for use in eq. 14 for the digital computer.

In the upper two graphs of fig. 6, we see that the experimental conditions are the same except for the presence and absence of surface roughness under idealized model conditions. When there was no surface roughness, it took the water stream 8 min to advance horizontally a distance = 157 cm on the surface of the porous media (see fig. 6 top left). When there was surface roughness created by spreading large glass beads on the surface of the fine beads, the stream has advanced horizontally a distance of 136 cm for the same time interval. For the same two experimental runs, the parameter C , which is the thickness of water on the surface, is not equal. We find that C was equal to 1.0 cm when there was no surface roughness, and C was equal to 1.3 cm, with surface roughness.

Fig. 9 shows the relation between the distance of advance and time for two identical runs except for the absence or presence of surface roughness. As seen in the figure, surface roughness influences the advance of water on a surface of 0-percent slope but not discernibly on a surface of 1-percent slope. Under model conditions, we find that the value of C with surface slope of 1 percent is about half the value of C when the surface was level (0-percent slope). This, in general, indicates that the parameter C reflects the hydraulic characteristics under the present experimental model runs.

Dimensionless Functions for the Horizontal Advance of Irrigation Water

The solution for the irrigation-advance problem, when the infiltration equation is given by $y = Et^\alpha$, may be written as (see eq. 14)

$$\frac{x}{q} = \frac{t}{C} \sum_{n=0}^{\infty} \frac{\{-Et^\alpha/C\}[\Gamma(1+\alpha)]^n}{\Gamma(2+na)}$$

with the terms defined as before. This equation is cumbersome to solve since the computer does not yield values for eq. 14 for large values of the quantity Et^α/C (see also Wilke and Smerdon, 1965) because

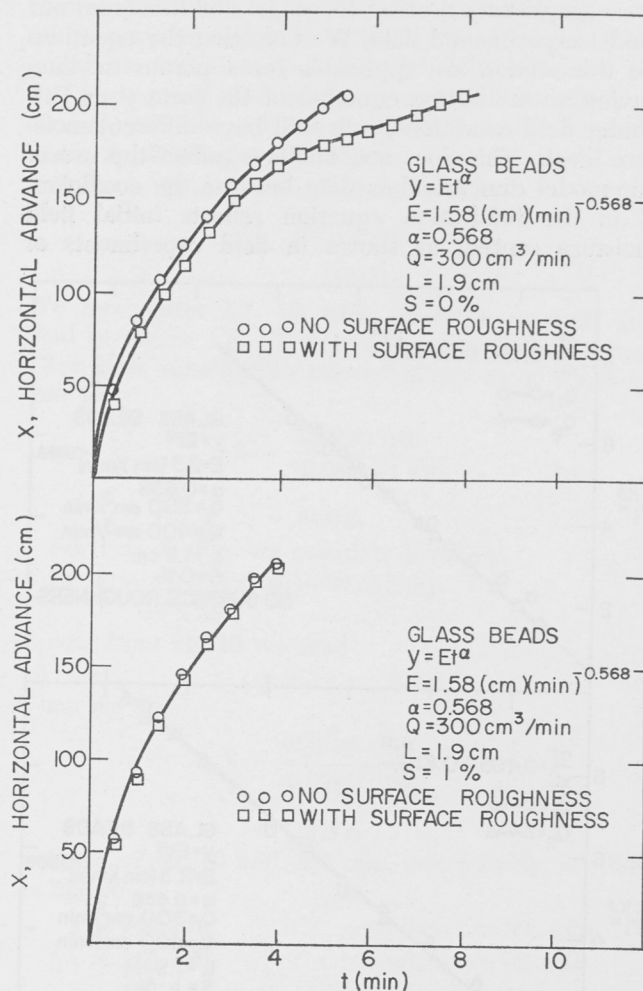


Fig. 9. The relation between horizontal distance of advance, with and without surface roughness when the surface slope is 0 percent and 1 percent and when glass beads are used.

of the slow convergence of the series. This equation can be rearranged as

$$\frac{Cx}{qt} = \sum_{n=0}^{\infty} \frac{[-Et^\alpha/C][\Gamma(1+\alpha)]^n}{\Gamma(2+na)}$$

This form of the equation is dimensionless in the quantities Cx/qt and Et^α/C . Our model experimental data, obtained by using idealized porous media (glass beads) with an infiltration equation of the form $y = Et^\alpha$, enables us to obtain dimensionless graphic solutions for eq. 14 beyond the range at which the computer failed to give appropriate solutions because of the slow convergence of the series.

Figs. 10-16 are plots of the dimensionless functions, and they fit straight lines for the different conditions of infiltration of the porous medium, different slopes and different surface roughnesses shown.

Equations of the form

$$\frac{qt}{Cx} = a + b \frac{Et^\alpha}{C}$$

were graphically derived for each condition from our model experimental data. We note that the equations for this section are applicable for a porous medium having an infiltration equation of the form $y = Et^\alpha$. Under field conditions, soils will have different moisture levels. This does not, however, affect the use of our model dimensionless data because the coefficient E in the infiltration equation reflects initial field moisture content as shown in field experiments of

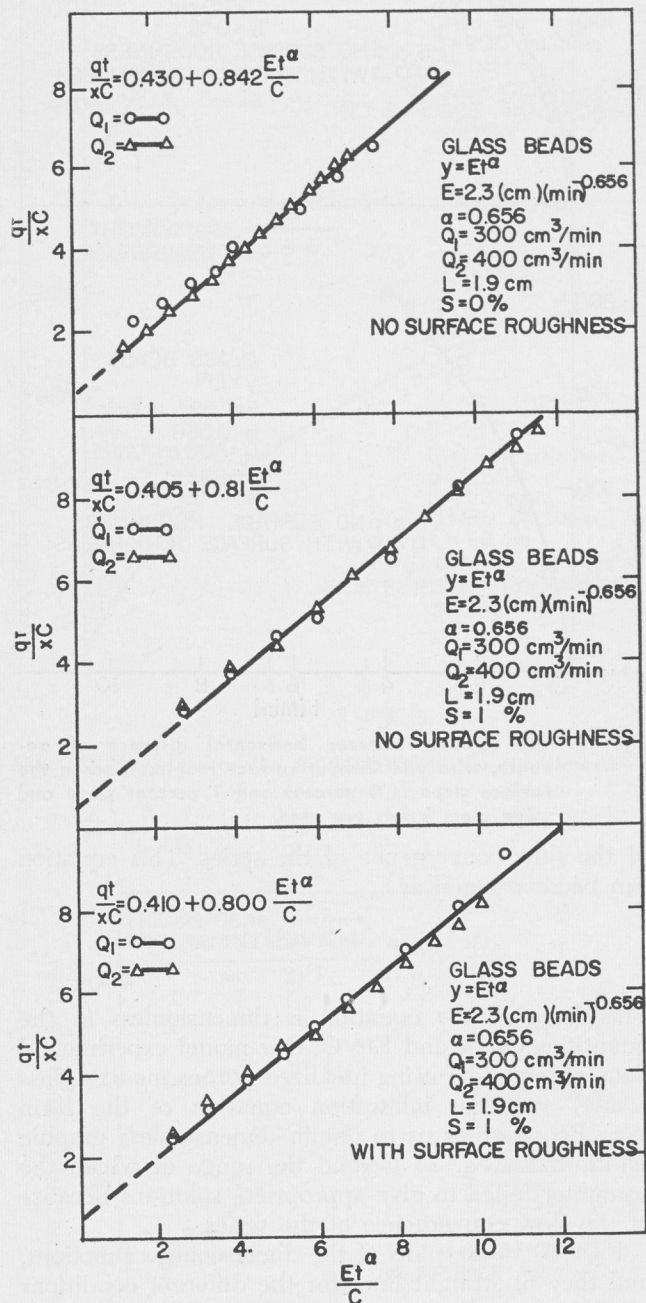


Fig. 10. Values of the dimensionless functions of qt/xC versus Et^α/C , calculated from the experimental runs in the model with glass beads the quantity t is the time for the water to advance on the surface a horizontal distance x . Each graph is a result of two independent runs with two different values of Q .

Toksöz et al. (1965). Since the quantity Et^α/C is dimensionless, the value of E obtained under field conditions will reflect the effect of initial moisture content.

We present a numerical example to demonstrate the use of the dimensionless model data. Suppose we have an irrigation system with field values given as follows: At the head of the irrigation check, water is introduced at a constant flow rate $q = 0.2735 \text{ m}^3/\text{m}/\text{min}$; the average depth of water on the soil is $C = 0.0381 \text{ m}$; the infiltration equation, known

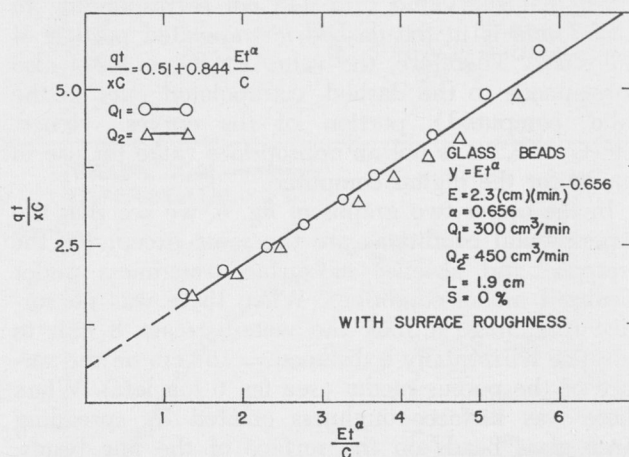


Fig. 11. The same as fig. 10, with different variables.

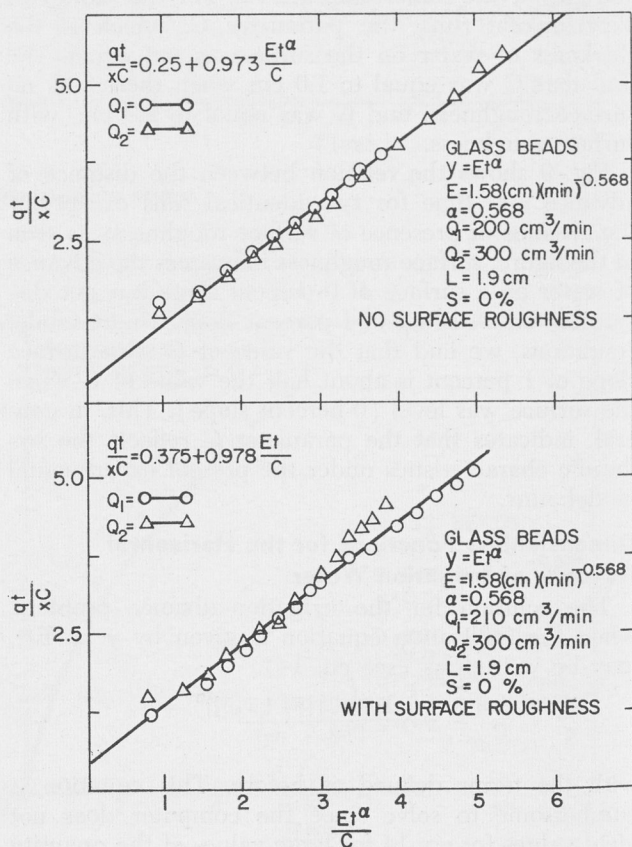


Fig. 12. The same as fig. 10, with different variables.

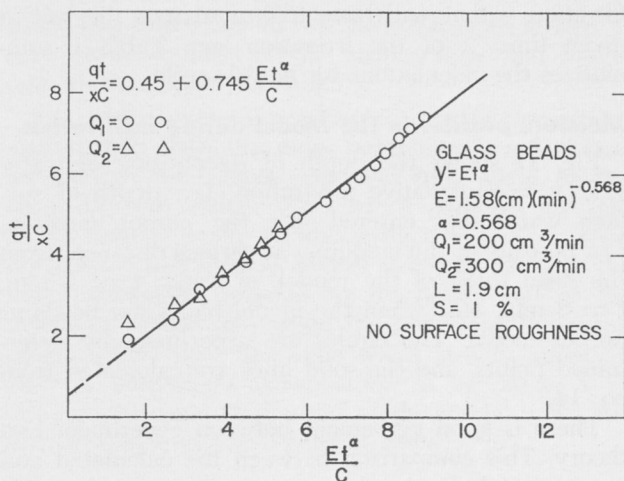


Fig. 13. The same as fig. 10, with different variables.

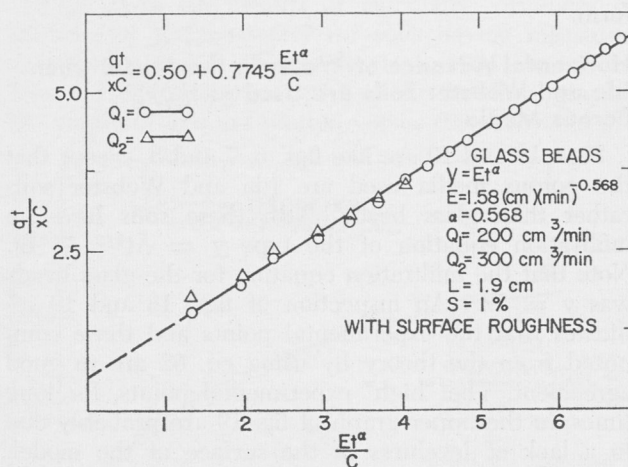


Fig. 14. The same as fig. 10, with different variables.

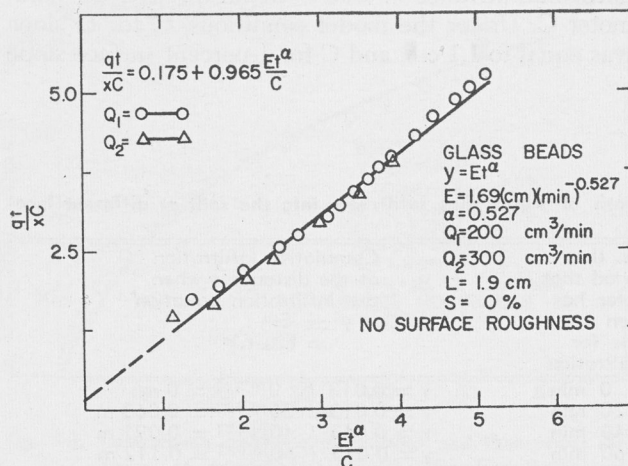


Fig. 15. The same as fig. 10, with different variables.

from experiments in the field, is $y = Et^\alpha$, where E and α are assumed to have been found as $\alpha = 0.527$ and $E = 0.0130$ (m) (min) $^{-0.527}$. We will solve for the position of the irrigation stream after 20 min, 40 min, 60 min, 80 min and 100 min of irrigation water application at the check.

For $t = 20$ min, we calculate Et^α/C as

$$Et^\alpha/C = \frac{(0.013)(20)^{0.527}}{0.0381} = 1.66$$

We now enter fig. 15 with $(Et^\alpha/C) = 1.66$ and read $qt/Cx = 1.77$. This last equality is then solved for x after substituting known values of q , t and C ; that is

$$X = \frac{(0.2735)(20)}{(0.0381)(1.770)}$$

$$= 81.0 \text{ m}$$

For $t = 40$ min, we calculate Et^α/C as

$$Et^\alpha/C = (0.013)(40)^{0.527}/0.0381 = 2.38$$

Again, from fig. 15 we read

$$(qt/Cx) = 2.40$$

Then we find

$$X = \frac{(0.2735)(40)}{(0.0381)(2.40)}$$

$$= 119.6 \text{ m}$$

For $t = 60, 80$ and 100 min, respectively, we find as before

$x = 142.9 \text{ m}$	when $t = 60 \text{ min}$
$x = 165.7 \text{ m}$	when $t = 80 \text{ min}$
$x = 177.8 \text{ m}$	when $t = 100 \text{ min}$

From our calculations we conclude: The position of the irrigation stream, s , will be 81.0 m, 119.6 m, 142.9 m, 165.7 m, and 177.8 m, after 20 min, 40 min, 60 min, 80 min and 100 min, respectively. These calculations will now enable us to further calculate, by using the equation $y = Et^\alpha$, the cumulative in-

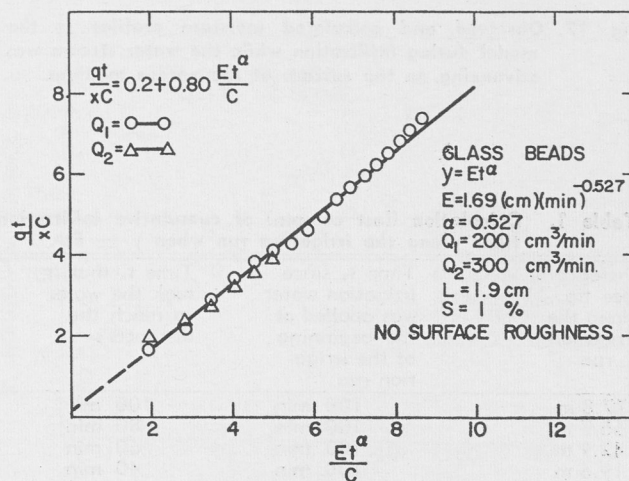


Fig. 16. The same as fig. 10, with different variables.

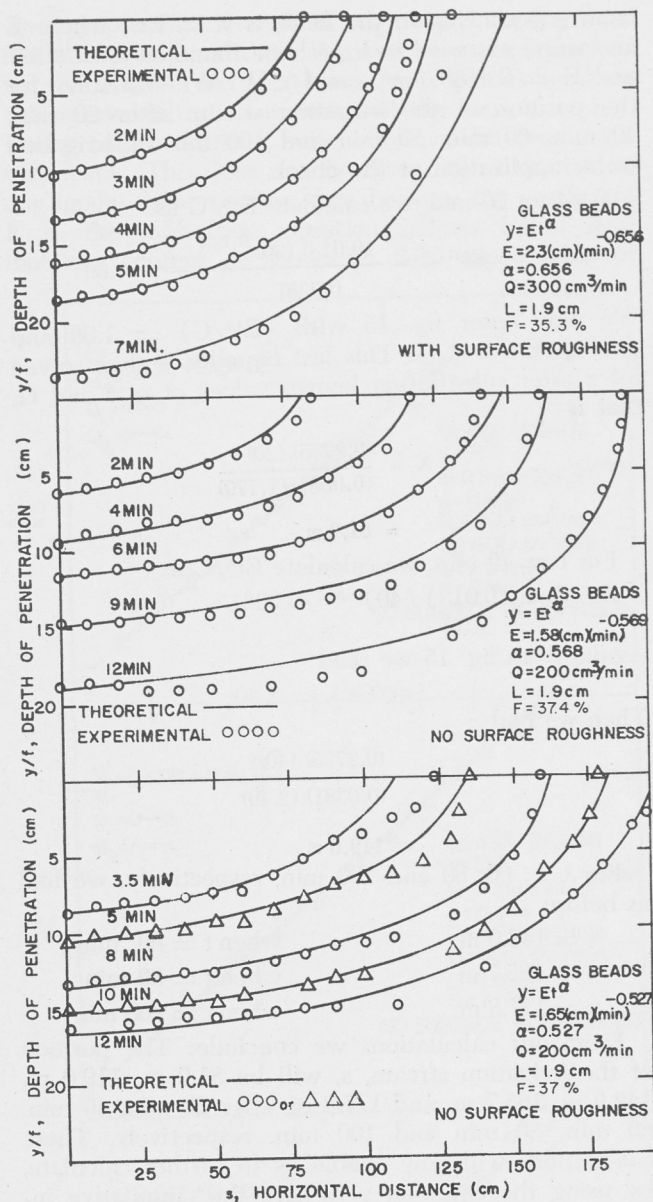


Fig. 17. Observed and calculated moisture profiles in the model during infiltration while the water stream was advancing on the surface of the porous medium.

filtration y that will have infiltrated into the soil at given times t of the irrigation run. Table 1 summarizes the calculations for our example.

Moisture profiles in the Model during Infiltration

Fig. 17 shows the depth of penetration of water y/f (y = cumulative infiltration; i.e., depth of surface water that entered into the porous medium, f = porosity of the medium) at various distances from the head ditch of the model, at times, $t = 2$ min, $t = 3$ min, etc., when the model had glass beads as porous media. The circles are experimentally determined points, and the solid lines are calculated from eq. 14.

There is good agreement between experiment and theory. This comparison between the calculated and experimental depth of penetration was not possible when the model had soils as porous media. This was because of the irregular distribution of soil-moisture content with depth. For the glass bead experiments, the moisture distribution with depth was nearly uniform.

Horizontal Advance of Water in the Model when Ida and Webster Soils are Used as the Porous Media

Figs. 18 and 19 are like figs. 6, 7 and 8, except that the porous media used are Ida and Webster soils rather than glass beads. Both these soils have an infiltration equation of the type $y = At^{1/2} + Bt$. Note that the infiltration equation for the glass beads was $y = Et^{\alpha}$. An inspection of figs. 18 and 19 indicates that the experimental points and those computed from the theory by using eq. 62 are in good agreement. The "high" experimental points, for long times, in the upper graph of fig. 19 are probably due to a lack of levelness of the surface of the model. The agreement between the experimental points and the theoretically computed curves, for both 0- and 1-percent slopes, indicates that the present theory takes into account the effect of surface slope on the horizontal advance of water stream through the parameter C . Under the model conditions, C for 0 slope was equal to 1.1 cm, and C for 1-percent surface slope

Table 1. Calculation (last column) of cumulative infiltration, (depth of water that infiltrates into the soil) at different locations along the irrigation run when $y = Et^{\alpha}$.

Distance s (see fig. 1) along the irrigation run	Time t_x since irrigation water was applied at the beginning of the irrigation run	Time t_s that it took the water to reach the distance s	$t_x - t_s$ the period that water has been available for infiltration	Cumulative infiltration at the distance s when the infiltration equation is $y = Et^{\alpha} = E(t_x - t_s)^{\alpha}$
177.8 m	100 min	100 min	0 min	$y = 0.013 (0)^{0.527} = 0$ m
165.7 m	100 min	80 min	20 min	$y = 0.013 (20)^{0.527} = 0.063$ m
142.9 m	100 min	60 min	40 min	$y = 0.013 (40)^{0.527} = 0.091$ m
119.6 m	100 min	40 min	60 min	$y = 0.013 (60)^{0.527} = 0.112$ m
81.0 m	100 min	20 min	80 min	$y = 0.013 (80)^{0.527} = 0.130$ m
0 m	100 min	0 min	100 min	$y = 0.013 (100)^{0.527} = 0.147$ m

was equal to 0.6 cm. As we have indicated before, C is a parameter fixed by the surface slope and roughness of the porous medium.

Fig. 20 shows the experimental data for two experimental runs with the same parameters, except that, for one run, the surface slope was zero, while, for the other run, the surface slope was 1 percent. The rate of advance of water on the surface increased when the surface had a slope greater than zero. It took the water stream 45 minutes to reach the end of the model ($x = 203$ cm) when the slope was 1 percent, but it would take the same water stream about 71 minutes (based on extrapolation in fig. 20 to $x = 203$ cm) to come to the end of the model when the surface was level (or 0-percent slope).

Theoretical Horizontal Advance of Irrigation Water When the Infiltration Equation is $y = At^{1/2} + Bt$ and the Parameters A and B are Determined under Field Conditions

Figs. 21-23 are results of calculated distances of advance of surface water for soils having measured values of A and B (Edwards et al., 1964) in the infiltration equation $y = At^{1/2} + Bt$. In these graphs, the values of x/q are plotted versus the time t , where

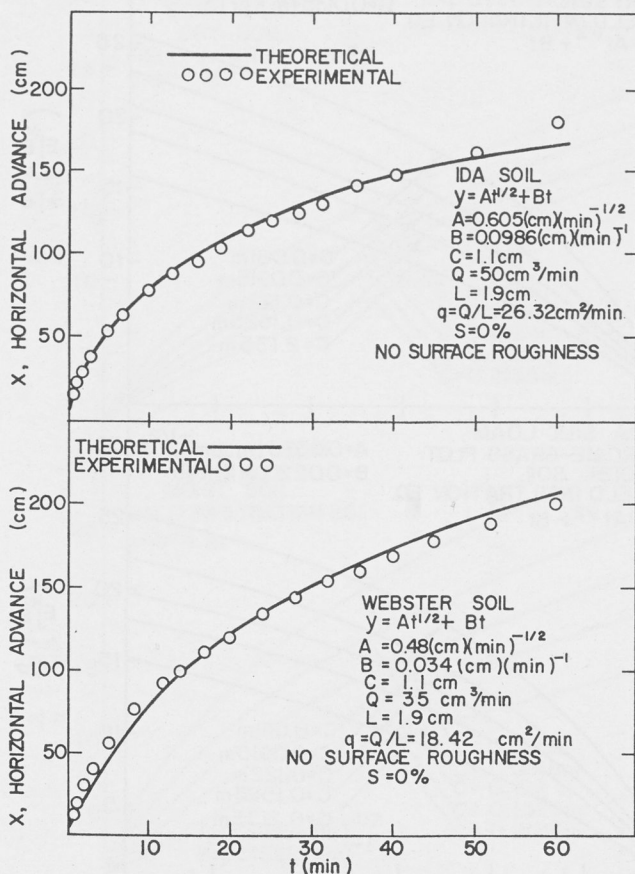


Fig. 18. Comparison of the experimental and theoretical distance of advance x of the "flooding irrigation" water on the porous medium surface in the model when Ida and Webster soil are used.

x is the horizontal distance in meters that the irrigation stream will advance in the field during surface irrigation and q is the amount of applied irrigation water per unit width per hr. The parameter C, the average depth of surface storage, will depend mainly on surface slope and roughness. When the infiltration rate is high, as in fig. 23 for Grundy soil, the rate of increase of the value x/q with time is small, and the family of curves is closer to each other.

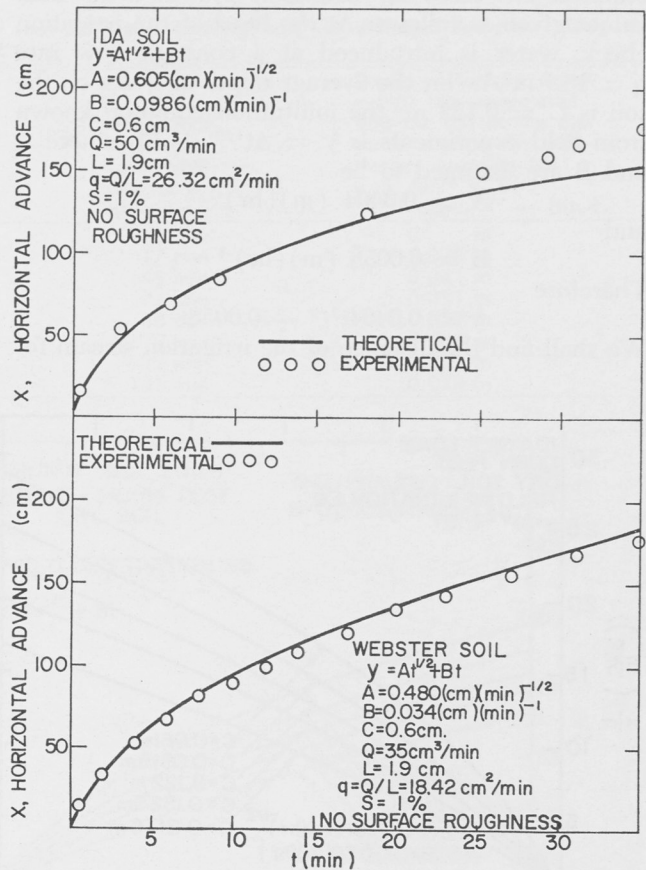


Fig. 19. The same as fig. 18 with different variables.

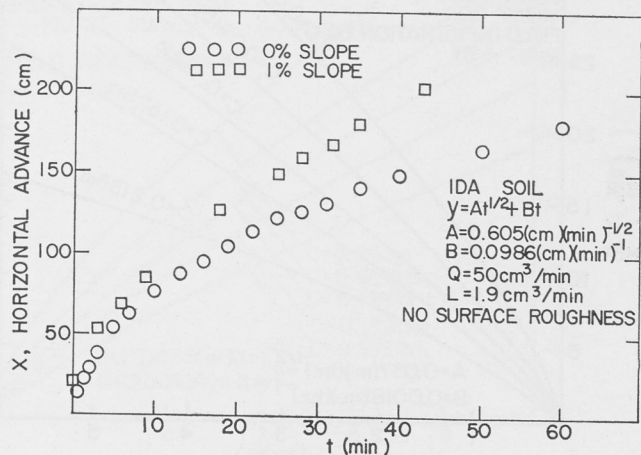


Fig. 20. Comparison of slopes of 0 and 1 percent on distance of advance of irrigation water for Ida soil.

The family of curves of figs. 21-23 could be used for other soil types if the measured cumulative infiltration equations are the same $y = At^{1/2} + Bt$ as the ones for which these theoretical curves were developed. In developing these families of curves, it is assumed that the soil is homogeneous throughout the irrigation check.

We now present a numerical example to demonstrate the use of the theoretical curves of figs. 21-23. Suppose we have an irrigation system with field values given as follows: At the head of the irrigation check, water is introduced at a constant flow rate $q = 15.1 \text{ m}^3/\text{m}/\text{hr}$; the average depth of water on the soil is $C = 0.122 \text{ m}$; the infiltration equation known from field experiments is $y = At^{1/2} + Bt$, where A and B are assumed to be

$$A = 0.0404 \text{ (m)(hr)}^{-1/2}$$

and

$$B = 0.0058 \text{ (m)(hr)}^{-1}$$

Therefore

$$y = 0.0404t^{1/2} + 0.0058t$$

We shall find the distance of the irrigation stream for

the following seven cases, after 13 min, 23 min, 47 min, 64 min, 87 min, 118 min and 135 min.

For $t = 13 \text{ min} = 0.217 \text{ hr}$, we enter the upper right graph of fig. 23 with $t = 0.217 \text{ hr}$ and read $(x/q) = 2.035 \text{ (m/m}^2)$.

Then we find

$$x = (2.035 \text{ m/m}^2)(15.1 \text{ m}^3/\text{m}) = 30.7 \text{ m}$$

Similarly for the other six cases we find

$x = 61.0 \text{ m}$	when $t = 23 \text{ min}$
$x = 91.4 \text{ m}$	when $t = 47 \text{ min}$
$x = 122.1 \text{ m}$	when $t = 64 \text{ min}$
$x = 152.5 \text{ m}$	when $t = 87 \text{ min}$
$x = 183.2 \text{ m}$	when $t = 118 \text{ min}$
$x = 207.2 \text{ m}$	when $t = 135 \text{ min}$

The advantage of the approach in this example is that we need not measure t versus x in the field for different rates of application q . Instead we measure the infiltration rate and then set up a design value for q . The need for this approach is indicated in Criddle (1949), Criddle and Davis (1951), Criddle et al. (1956), Israelson (1962), Lewis (1937), Beer (1957),

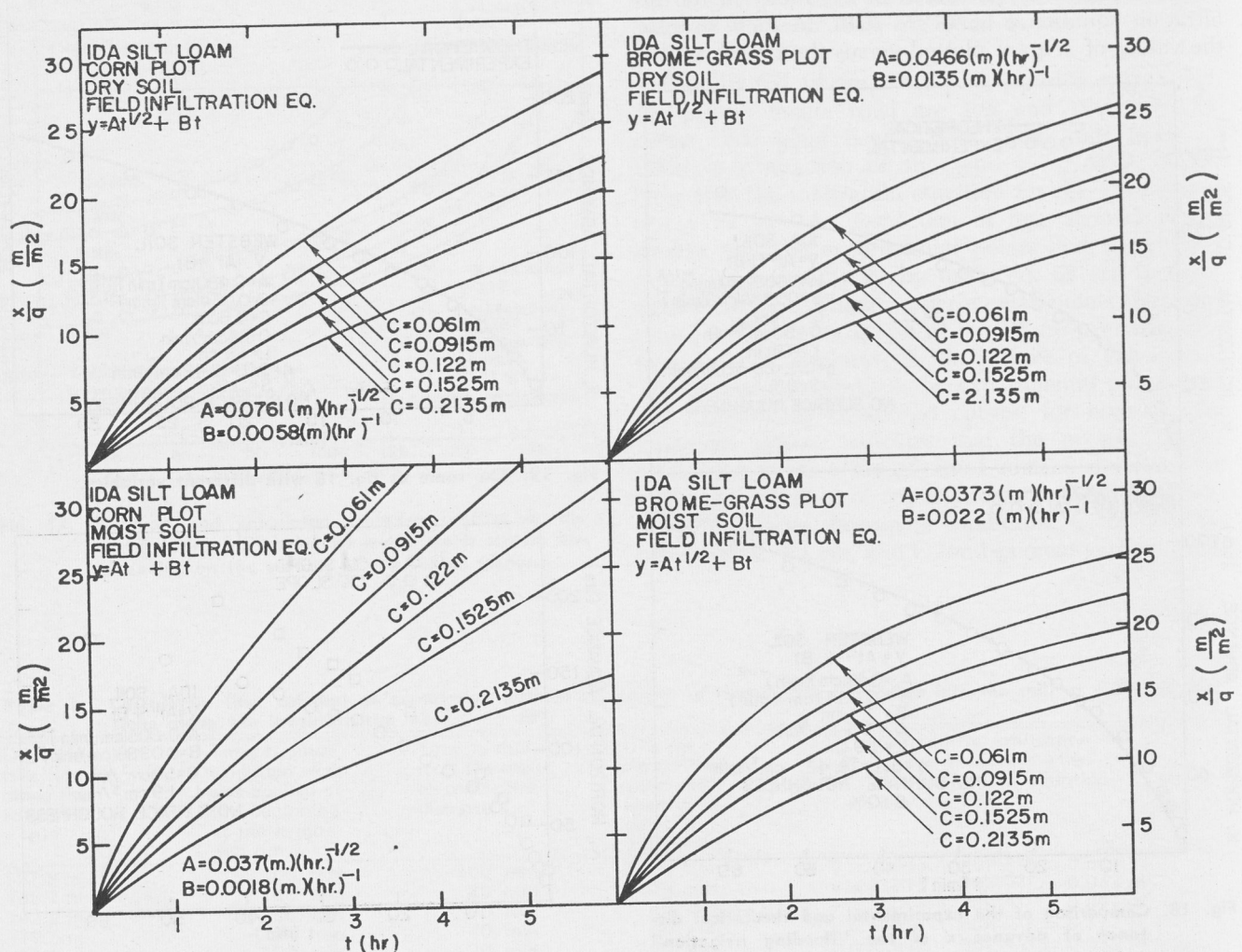


Fig. 21. Calculated distances of advance of irrigation water for several shown values of coefficients, A and B , for Ida soil.

Smerdon (1963) and Smerdon and Hohn (1961). In our examples, the calculation of the position of the irrigation stream allows us to know how long water will pond on the surface and how much water will infiltrate into the soil at each location. Table 2 summarizes calculations for our example.

In this example, we assumed a value of 0.122 m for C. To demonstrate the effect of the parameter C on the distance of advance of the water stream on

the surface, let us now consider another example where we have the same infiltration equation and the design value of q as in the example just given, but instead of C = 0.122 m, we will assume a value of C = 0.2135 m. We shall again find the advance of the irrigation stream for the following seven cases; after 13 min, 23 min, 47 min, 64 min, 87 min, 118 min and 135 min.

For t = 13 min = 0.217 hr, we enter the upper

Table 2. Calculation of cumulative infiltration (depth of water that infiltrates into the soil) at different locations along the irrigation run when $y = At^{1/2} + Bt$, and C = 0.122 m.

Distance s (see fig. 1) along the irrigation run	Time t_x since irrigation water was applied at the beginning of the irrigation run	Time t_s that it took the water to reach the distance s	$t_x - t_s$ the period that water has been available for infiltration	Depth of surface water y that has penetrated into the soil at the distance s when the infiltration equation is $y = At^{1/2} + Bt = A(t_x - t_s)^{1/2} + B(t_x - t_s)$
207.2 m	135 min	135 min	0 min	0 m
183.2 m	135 min	118 min	17 min	0.025 m
152.5 m	135 min	87 min	48 min	0.041 m
122.1 m	135 min	64 min	71 min	0.051 m
91.4 m	135 min	47 min	88 min	0.057 m
61.0 m	135 min	23 min	112 min	0.066 m
30.7 m	135 min	13 min	122 min	0.070 m
0 m	135 min	0 min	135 min	0.074 m

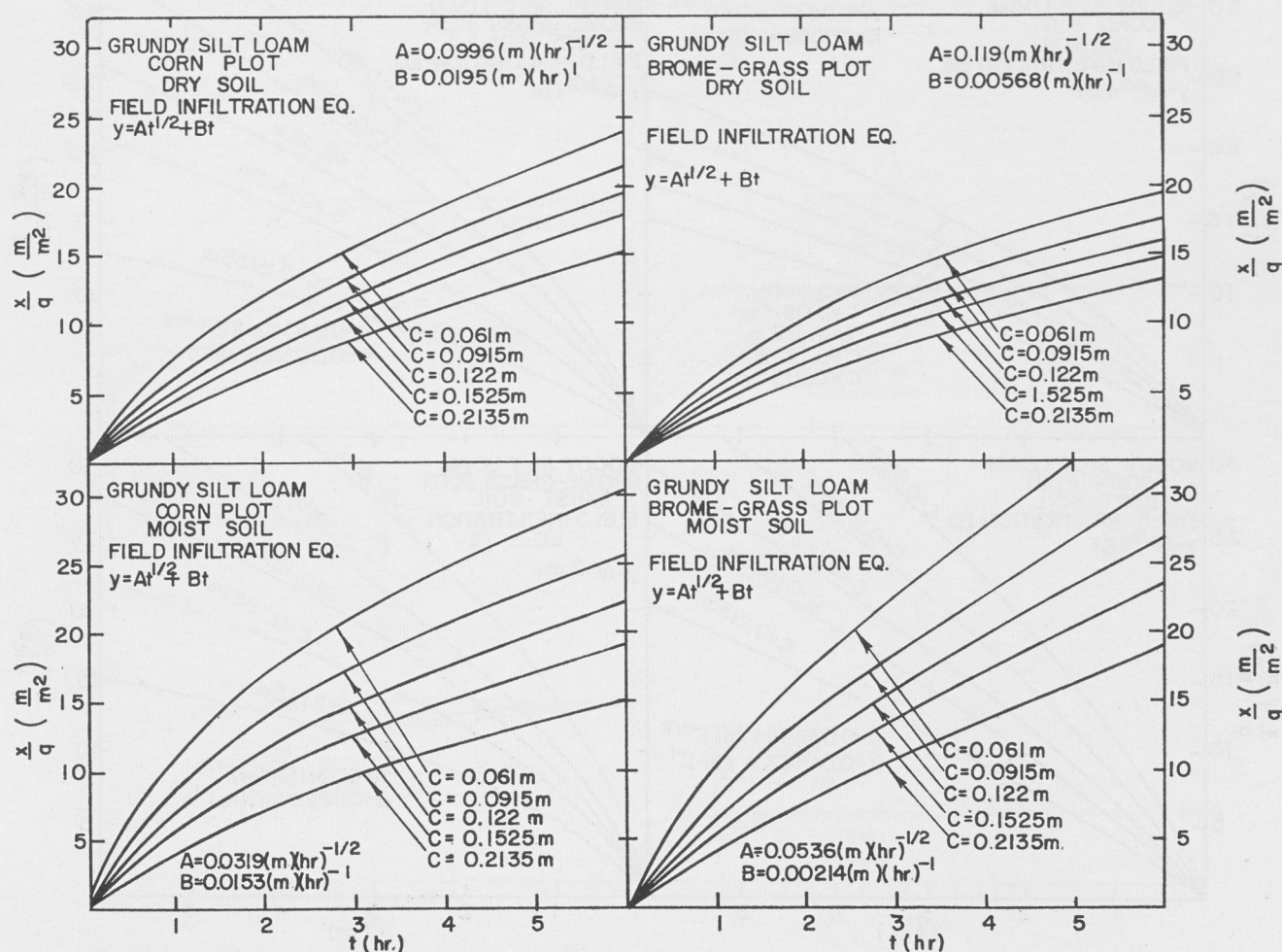


Fig. 22. Same as fig. 21 except for Grundy soil.

right graph of fig. 23 with $t = 0.217$ hr and read $x/q = 0.825$ (m/m^2) for the case when the infiltration equation is $y = 0.0404t^{1/2} + 0.0058t$, and $C = 0.2135$ m.

Then we find

$$x = (0.825) (15.1m^3/m) = 12.41 \text{ m}$$

Similarly, for the other six cases we find:

$x = 24.3$ m	when $t = 23$ min
$x = 47.7$ m	when $t = 47$ min
$x = 58.0$ m	when $t = 64$ min
$x = 77.4$ m	when $t = 87$ min
$x = 92.6$ m	when $t = 118$ min
$x = 99.5$ m	when $t = 135$ min

For this example, the numerical values of the cumulative infiltration of the water into the soil at the given distances of advance after 135 min are: at zero distance, 0.074 m of water; at 12.41 m, 0.070 m; at 24.3 m, 0.066 m; at 47.7 m, 0.057 m; at 58.0 m, 0.051 m; at 77.4 m, 0.0410 m; at 92.6 m, 0.025 m and at 99.5 m, zero.

Theoretical Horizontal Advance of Irrigation Water When the Infiltration Equation is $y = Kt$, as for Sand

In sandy soils, the infiltration equation is of the type $y = Kt$, the K factor in this equality is the slope of the straight line when y is plotted versus t . This K factor is equal to the Darcy law K for the sand where capillary effects are negligible.

Fig. 24 shows theoretical curves of x/q versus t . These theoretical curves are for different values of K in $y = Kt$ and for different depths of surface water thickness C . These graphs should prove useful in irrigation design to calculate the maximum allowable length of irrigation run for a minimum deep-seepage loss.

We recall (see eq. 12) that the solution for the irrigation equation when infiltration is given by $y = Kt$ is

$$x(t) = \frac{q}{K} [1 - e^{-(K/C)t}]$$

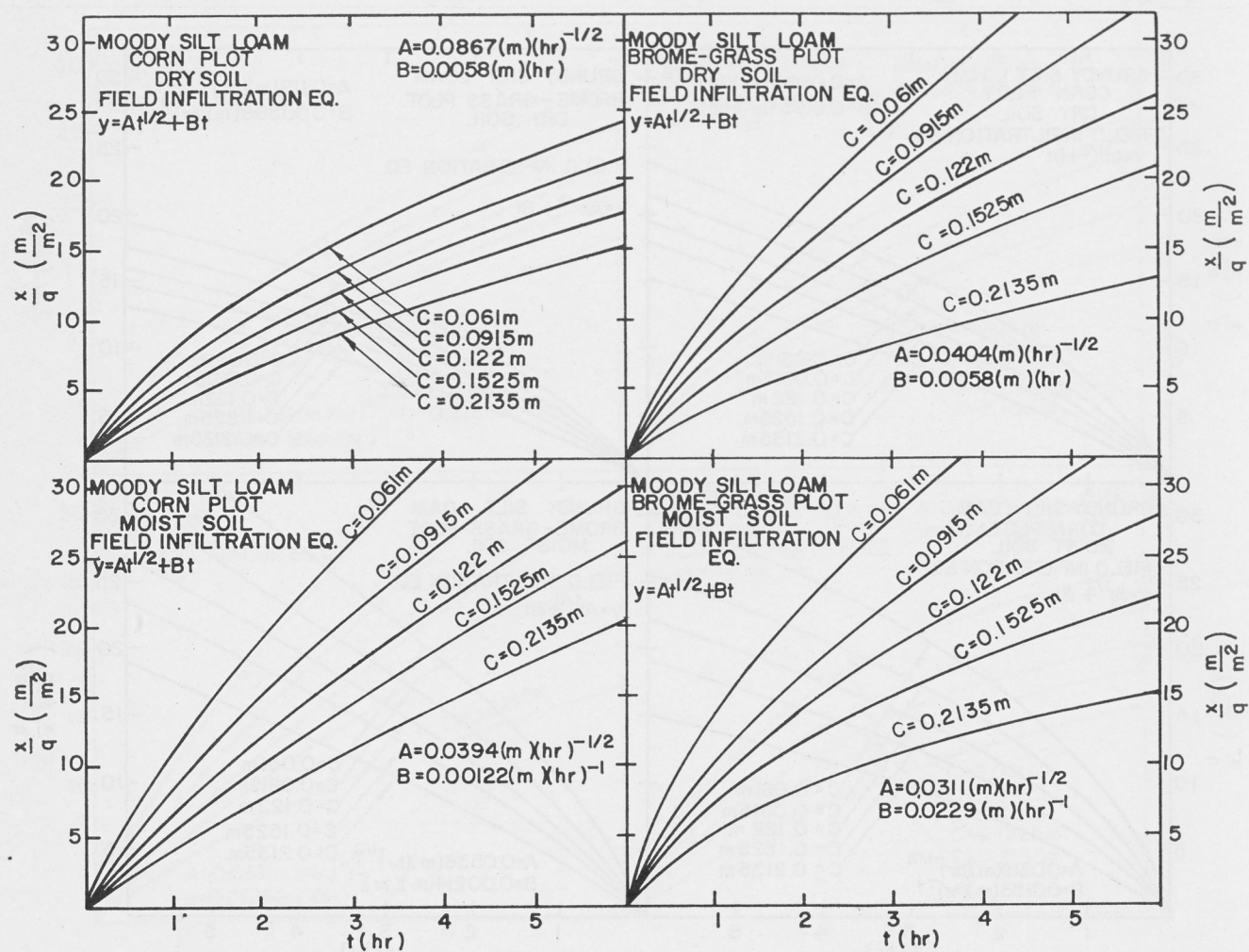


Fig. 23. Same as fig. 21 except for Moody soil.

where we recall and emphasize that, for $y = Kt$, there is a mathematically exact maximum distance of advance given by the expression

$$\lim_{t \rightarrow \infty} x(t) = q/K$$

This expression shows that when we apply a constant amount of irrigation water q at the head of the irrigation check, then the maximum distance of advance is equal to the ratio q/k , regardless of the depth of surface storage C . We present a numerical example similar to the examples given before, except that the soil in this instance has an infiltration equation of the type $y = Kt$. Suppose we have an irrigation system with field values given as follows: At the head of the irrigation check, water is introduced at constant flow rate $q = 13.95 \text{ (m}^3/\text{m)}/\text{hr}$, the average depth of the water on the soil is $C = 0.0915 \text{ m}$; the infiltration equation known from experiments in the field is $y = Kt$, where K is assumed to have been found as $K = 0.2 \text{ m/hr}$. We will solve for the position of the irrigation stream for the following six cases, after 20 min, 40 min, 60 min, 80 min, 100 min and 120 min.

For $t = 20 \text{ min} = 0.333 \text{ hr}$, we enter the lower right graph of fig. 24 with $t = 0.333 \text{ hr}$ and read $x/q = 2.55 \text{ (m/m}^2\text{)}$. Because our design q value is given as $q = 13.95 \text{ (m}^3/\text{m)}/\text{hr}$, we find that

$$x = (2.55) (13.95) = 35.6 \text{ m}$$

Similarly for the other five cases we find the following results:

$x = 53.5 \text{ m}$	when $t = 40 \text{ min}$
$x = 62.0 \text{ m}$	when $t = 60 \text{ min}$
$x = 65.8 \text{ m}$	when $t = 80 \text{ min}$
$x = 67.9 \text{ m}$	when $t = 100 \text{ min}$
$x = 68.7 \text{ m}$	when $t = 120 \text{ min}$

We find also that the maximum distance of advance in this example is

$$\begin{aligned} x(\text{maximum}) &= q/K \\ &= 13.95/0.20 \\ &= 69.75 \text{ m} \end{aligned}$$

This calculation of the position of the irrigation stream allows us to know how long water will pond on the surface at each location and how much water will infiltrate into the soil. Such calculations (see table 1 for the method of calculation) show that cumulative in-

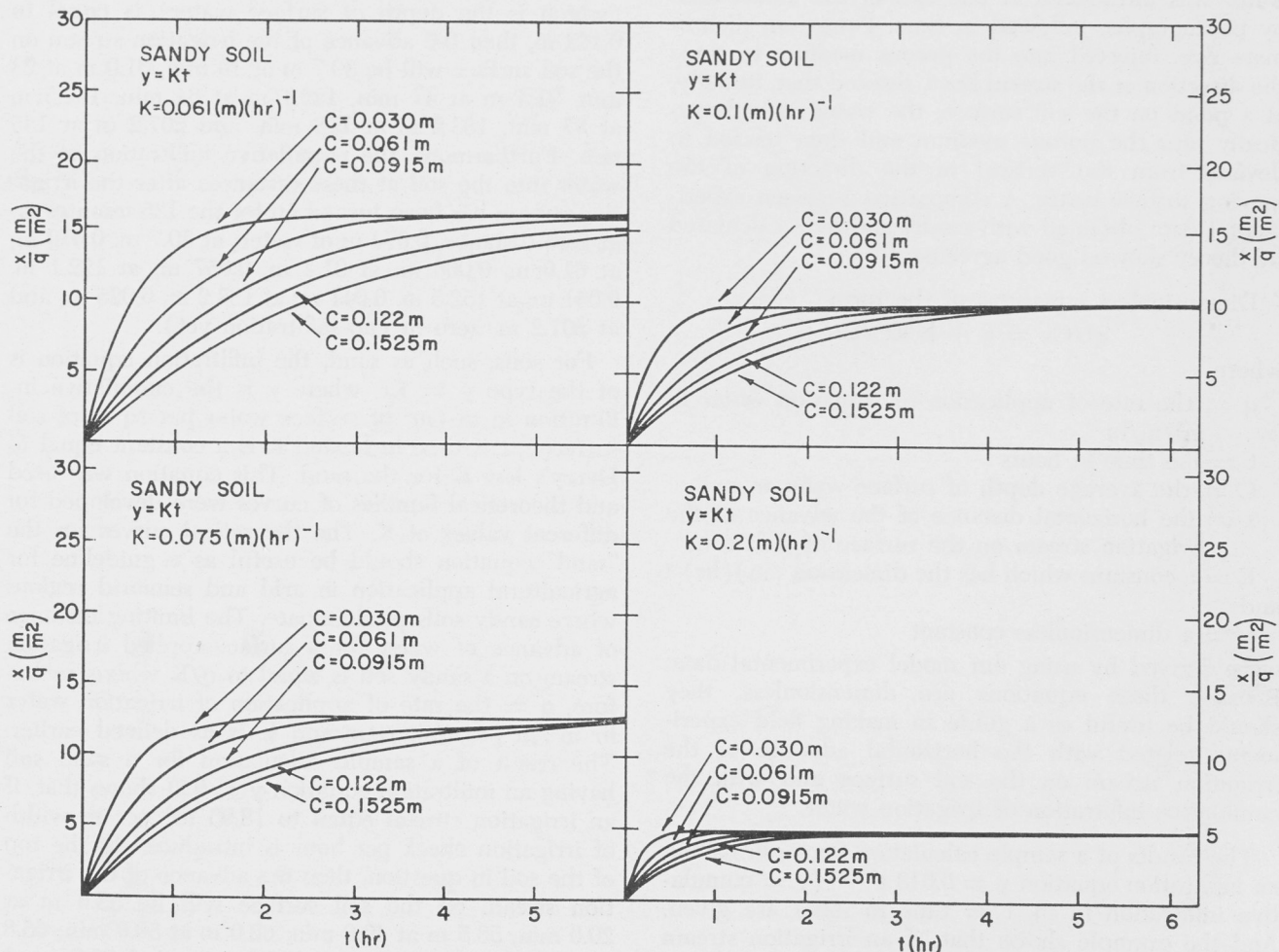


Fig. 24. Theoretical curves for the quantity x/q versus t for sandy soils. The curves are developed for different values of K , assuming the field infiltration equation is $y = Kt$.

filtration of the water into the soil at the given distances of advance after the irrigation stream has been turned on for 120 min is: at zero distance, 0.400 m of water; at 35.6 m, 0.333 m; at 53.5 m, 0.266 m; at 62.0 m, 0.20 m; at 65.8 m, 0.133 m; at 67.9 m, 0.067 m and at 68.7 m, zero.

DISCUSSION

Mathematical equations describing the horizontal advance of the irrigation stream on the surface of soil have been derived and discussed for various types of infiltration equations corresponding to different field conditions. Complex-variable theory was applied to transform certain complicated forms of solutions to solutions in algebraic form that could be used easily in irrigation design.

A laboratory model for testing the theory was made. The model had glass beads, or soil aggregates, as the porous medium and had water as fluid and walls of transparent Plexiglas through which water on the surface of the porous medium or in the porous medium could be photographed. "Flooding irrigation" water was introduced at one end of the model and, by photographs, followed in time. Potassium dichromate dye, injected into the porous medium to trace the direction of the stream lines, showed that, initially, at a point on the soil surface, the water moved vertically into the porous medium and then tended to deviate from the vertical in the direction of the moving surface water. A comparison between experimental data obtained with model and data calculated by theory showed good agreement.

Dimensionless equations of the form

$$qt/Cx = a + b Et^\alpha/C$$

where

q = the rate of application of irrigation water in $m^3/m/hr$

t = the time in hours

C = the average depth of surface water in m

x = the horizontal distance of the advance of the irrigation stream on the surface of soil in m

E = a constant which has the dimension $(m)(hr)^\alpha$ and

α = a dimensionless constant

were derived by using our model experimental data. Because these equations are dimensionless, they should be useful as a guide in making field experiments related with the horizontal advance of the irrigation stream on the soil surface and with the cumulative infiltration of irrigation water.

The results of a sample calculation for a soil having an infiltration equation $y = 0.013 t^{0.527}$ (y = cumulative infiltration in m, t = time in min) are given. And the example shows that, if an irrigation stream of amount $0.2755 m^3$ per m width of irrigation run per min is introduced at the top of a field of the soil in

question, then the advance of the irrigation stream on the soil surface will be 81.0 m at 20 min, 119.6 m at 40 min, 142.9 m at 60 min, 165.7 m at 80 min and 177.8 m at 100 min. Furthermore, the cumulative infiltration of the water into the soil at these several distances after the irrigation stream has been turned on for the 100 minutes is: at zero distance, 0.1470 m of water penetration; at 81.0 m, 0.130 m; at 119.6 m, 0.112 m; at 142.9 m, 0.091 m; at 165.7 m, 0.063 m; and at 177.8 m, zero m (no infiltration yet).

To apply the theory to field soils that have an infiltration equation of the type $y = At^{1/2} + Bt$, where the parameters A and B are determined under different soil conditions, families of curves were developed and were applied in some field-irrigation problems. The results of a sample calculation for a soil having an infiltration equation

$$y = 0.0404 t^{1/2} + 0.0058 t$$

(y = cumulative infiltration in m, t = time in hr) shows that, if an irrigation stream of amount $15.1 m^3$ per m width of irrigation check per hr is introduced at the top of a field of the soil in question and if C (which is the depth of surface water) is equal to 0.122 m, then the advance of the irrigation stream on the soil surface will be 30.7 m at 13 min, 61.0 m at 23 min, 91.4 m at 47 min, 122.1 m at 64 min, 152.5 m at 87 min, 183.2 m at 118 min, and 207.2 m at 135 min. Furthermore, the cumulative infiltration of the water into the soil at these distances after the irrigation stream has been turned on for the 135 minutes is: at zero distance, 0.074 m of water; at 30.7 m, 0.070 m; at 61.0 m, 0.066 m; at 91.4 m, 0.057 m; at 122.1 m, 0.051 m; at 152.5 m, 0.041 m; at 183.2 m, 0.025 m; and at 207.2 m, zero m (no infiltration yet).

For soils, such as sand, the infiltration equation is of the type $y = Kt$, where y is the cumulative infiltration in m (m^3 of surface water per sq m of soil surface), t is time in hr and K is a constant equal to Darcy's law K for the sand. This equation was used and theoretical families of curves were developed for different values of K . The theoretical curves for the "sand" equation should be useful as a guideline for agricultural application in arid and semiarid regions where sandy soils predominate. The limiting distance of advance of water for a surface-applied irrigation stream on a sandy soil is equal to q/K where, as before, q = the rate of application of irrigation water in m^3/m per unit time and K is as defined earlier. The result of a sample calculation for a sand soil having an infiltration equation $y = 0.2t$ shows that, if an irrigation stream equal to $13.95 m^3$ per m width of irrigation check per hour is introduced at the top of the soil in question, then the advance of the irrigation stream on the soil surface will be 35.6 m at 20.0 min; 53.5 m at 40.0 min; 62.0 m at 50.0 min; 65.8 m at 80.0 min, 67.9 m at 100.0 min; and 68.7 m at 120.0 min. Furthermore cumulative infiltration of the

water into the soil at these distances after the irrigation stream has been turned on for 120 min is: at zero distance, 0.40 m of water; at 35.6 m, 0.333 m;

at 53.5 m, 0.266 m; at 62.0 m, 0.20 m; at 65.8 m, 0.133 m; at 67.9 m, 0.067 m; and at 68.7 m, 0 m (no infiltration yet).

BIBLIOGRAPHY

- Abramowitz, M., and I. A. Stegun. (eds.) 1964. Handbook of mathematical functions. National Bureau of Standards, U. S. Department of Commerce, Washington, D. C.
- Beer, C. E. 1957. Infiltration and flow characteristics as applied to furrow irrigation design in Iowa. Unpublished M.S. thesis. Library, Iowa State University of Science and Technology, Ames.
- Chen, Cheng-lung. 1966. Discussion on a solution of the irrigation advance problem by O. Wilke and E. T. Smerdon. Amer. Soc. Civ. Eng. Jour. Irrig. Drain Div. Separate 4829, Vol. 91, No. IR2, pp. 97-101.
- Churchill, R. V. 1941. Fourier series and boundary value problems. McGraw-Hill Co., Inc. New York, N. Y.
- . 1958. Operational mathematics. 2nd ed. McGraw-Hill Co., Inc. New York, N. Y.
- . 1960. Complex variables and applications. 2nd ed. McGraw-Hill Co., Inc. New York, N. Y.
- Criddle, W. D. 1949. A practical method of determining proper lengths of runs, sizes of furrow streams and spacing of furrows on irrigated lands. Soil Conservation Service, U. S. Department of Agriculture. (Multilith) Washington, D.C.
- , and S. Davis. 1951. A method for evaluating border irrigation layouts. Soil Conservation Service, U.S. Department of Agriculture (Multilith) Washington, D.C.
- , S. Davis, C. Pair and D. Shockley. 1956. Methods for evaluating irrigation systems. Soil Conservation Service, U.S. Department of Agriculture Handbook 82. Washington, D.C.
- Edwards, W. M., R. G. Palmer, W. E. Larson and M. Amemiya. 1964. Annual report of cooperative regional projects, Project NC-40, Water infiltration into soils. (Mimeo.) Department of Agronomy, Iowa State University of Science and Technology, Ames.
- Faddeyeva, V. N., and N. M. Terentev. 1961. Tables of values of the functions $w(z)$ for a complex argument. (English translation). Pergamon Press, New York, N. Y.
- Fulks, W. 1962. Advanced calculus. (Esp. pp. 340-349) John Wiley and Sons, Inc., New York, N.Y.
- Grover, B. L., and Don Kirkham. 1964. Solving tile drainage problems by use of model data. Iowa Agr. and Home Econ. Exp. Sta. Res. Bul. 523.
- Hille, E. 1959. Analytic function theory. Vol. 1. Ginn and Company, New York, N.Y.
- Hodgman, C. D., R. C. Weast, R. S. Shankland and S. M. Selby. (eds.) 1957-1958. Handbook of chemistry and physics. 39th ed. The Chemical Rubber Publishing Co., Cleveland, Ohio.
- Holl, D. L., C. G. Maple and B. Vinograde. 1959. Introduction to the Laplace transform. Appleton Century Crofts, Inc. New York, N.Y.
- Israelson, O. W. 1962. Irrigation principles and practices. 3rd ed. John Wiley and Sons, New York, N.Y.
- Kirkham, Don. 1940. Pressure and streamline distribution in water-logged land overlying an impervious layer. Soil Sci. Soc. Amer. Proc. 5:65-68.
- Lewis, M. R. 1937. The rate of infiltration of water in irrigation practices. Amer. Geophys. Union Trans. 18:361-368.

- , and W. E. Milne. Analysis of border irrigation. 1938. *Agr. Eng.* 19:267-272.
- Philip, J. R. 1957a. Numerical solution of equations of the diffusion type with diffusivity concentration dependence. II. *Aust. Jour. Phys.* 10:29-42.
- , 1957b. The theory of infiltration. I. The infiltration equation and its solution. *Soil Sci.* 83:345-357.
- , 1957c. The theory of infiltration. II. The profile at infinity. *Soil Sci.* 83:435-448.
- , 1957d. The theory of infiltration. III. Moisture profiles and relation to experiment. *Soil Sci.* 84:163-178.
- , 1957e. The theory of infiltration. IV. Sorptivity and algebraic infiltration equations. *Soil Sci.* 84:257-264.
- , 1957f. The theory of infiltration. V. The influence of the initial moisture content. *Soil Sci.* 84:329-339.
- , 1958a. The theory of infiltration. VI. Effect of water depth over soil. *Soil Sci.* 85:278-286.
- , 1958b. The theory of infiltration. VII. *Soil Sci.* 85:333-337.
- , and D. A. Farrell. 1964. General solution of the infiltration-advance problem in irrigation hydraulics. *Jour. Geophys. Res.* 69:621-631.
- Smerdon, E. T. 1963. Subsurface water distribution in surface irrigation. *Amer. Soc. Civ. Eng. Jour. Irrig. Drain. Div. Separate 3441*, Vol. 89, No. IR 1, pp. 1-15.
- , and C. M. Hohn. 1961. Relationship between the rate of advance and intake rate in furrow irrigation. *Texas Agr. Exp. Sta. Misc. Pub.* 509.
- Toksöz, S., Don Kirkham and E. R. Baumann. 1965. Two-dimensional infiltration and wetting fronts. *Amer. Soc. Civ. Eng. Jour. Irrig. Drain. Div. Separate 4474*, Vol. 91, No. IR 3, pp. 65-79.
- Wilke, O., and E. T. Smerdon. 1965. A solution of the irrigation advance problem. *Amer. Soc. Civ. Eng. Jour. Irrig. Drain. Div. Separate 4471*, Vol. 91, No. IR 3, pp. 23-24.



